PEOPLE'S DEMOCRATIC REPUBLIC OF ALGERIA MINISTRY OF HIGHER EDUCATION AND SCIENTIFIC RESEARCH

SAAD DAHLAB UNIVERSITY OF BLIDA 1 FACULTY OF SCIENCE



Final project for obtaining a Master's degree

Sector: Chemistry

Specialty: Organic Chemistry

Theme

Preparation and characterization of activated carbon and application to pollutant adsorption: kinetic, isotherm, and dynamic studies

Presented by:

Abdenasser BOUMESSAIDIA

Dr Hamza .K	USDB1	President
Dr Bessi .A	USDB1	Examiner
Dr Chini .Z	USDB1	Promoter

Appreciation

First of all, we thank God for giving us the strength to complete our studies and accomplish this modest project.

We would like to thank Dr. Chini for agreeing to supervise this project, and Dr. Boumessaidia for his guidance and invaluable assistance.

We thank Dr Bessi .A and Dr Hamza .K for agreeing to judge our work.

Our sincere gratitude goes to our professors in the Department of Chemistry.

dedication

I dedicate this modest work to my dear father my dear mother, and my brothers, and my sisters for their support throughout my student years.

As well as to my friends who have always been there during difficult times.

Abstract:

The primary purpose of this study is to look at how activated carbon can be used to decontaminate dye-polluted water (methyl blue and methyl orange). We talked about theoretical water contamination, colorants, and adsorption. The materials, products, and experimental techniques, as well as the methods utilized to prepare activated carbon, have all been thoroughly detailed.

We have discussed the characteristics of activated carbon: infrared spectroscopy (IR) reveals the presence of C \equiv C, C \equiv C, C \equiv C, C \equiv O and C \equiv H groups. The observations made correspond to the pseudo-first-order and pseudo-second-order kinetic equations, with an excellent fit for the second and first orders. The Langmuir model illustrates the adsorption isotherms more effectively compared to the Freundlich model. The thermodynamic parameters suggest that the adsorption is endothermic (Δ H \geqslant 0).

Keywords: water pollution, Activated carbon, Methylene Blue, Methyl Orange, adsorption, kinetics, isotherm, thermodynamics.

الملخص:

يهدف هذا العمل في المقام الأول إلى دراسة إزالة تلوث المياه الملوثة بالأصباغ (أزرق الميثيلين وبرتقال الميثيل) باستخدام الكربون المنشط. المنشط. استعرضنا نظريًا تلوث المياه، والامتزاز، والكربون المنشط. وُصفت المواد والمنتجات والإجراءات التجريبية، بما في ذلك تحضير الكربون المنشط والتقنيات المستخدمة، بعناية. ناقشنا خصائص الكربون المنشط: يكشف التحليل الطيفي بالأشعة تحت الحمراء (IR) عن وجود مجموعات C=C و C=C و C=C و C=C تتوافق الملاحظات التي تم إجراؤها مع معادلات الحركية من الدرجة الأولى الزائفة والدرجة الثانية الزائفة، مع ملاءمة لا تشوبها شائبة للرتبتين الثانية والأولى. يوضح نموذج لانجموير بشكل أكثر فعالية خطوط الامتزاز المتساوية الحرارة مقارنةً بنموذج فروندليش. تشير المعلومات الديناميكية الحرارية إلى أن الامتزاز ماص للحرارة (Δ H>O).

الكلمات المفتاحية: المياه الملوثة، الكربون المنشط، أزرق الميثيلين، برتقالي الميثيل، الامتزاز، الحركية، خط الامتزاز المتساوي الحرارة. الديناميكا الحرارية

Résumé:

Ce travail vise principalement à examiner la dépollution d'une eau contaminée par des colorants (Bleu de méthylène et Orange de méthyle) en utilisant du charbon actif. Nous avons rappelé théoriquement, la contamination des eaux, l'adsorption et le charbon active. Les matériaux, les produits et les procédures expérimentales, y compris la préparation du charbon actif et les techniques employées, ont été soigneusement décrits.

Nous avons abordé les caractéristiques du charbon actif : spectroscopie infrarouge (IR) révèle la présence de groupements $C\equiv C$, C=C, C=C et C-H. Les observations réalisées correspondent aux équations cinétiques du pseudo-premier ordre et du pseudo-second ordre, avec un ajustement impeccable pour le second et le premier ordre. Le modèle de Langmuir illustre plus efficacement les isothermes d'adsorption en comparaison au modèle de Freundlich. Les paramètres thermodynamiques suggèrent que l'adsorption se fait avec un caractère endothermique ($\Delta H>0$).

Mots-clés: Eau polluée, Charbon actif, Bleu de méthylène, Orange de méthyle, adsorption, cinétique, isotherme, thermodynamique.

List of abbreviations:

- **AC:** Activated Carbon.
- **MW:** Microwave.
- **ZICNSC**: Zirconium impregnated Cashew nutshell AC.
- **GHG:** greenhouse gases.
- **BET**: Brunauer–Emmett–Teller.
- **BM:** Methylene blue.
- **OM:** Methyl Orange.
- **UV:** Ultraviolet.
- **FTIR:** Fourier Transform Infrared Spectroscopy.

List of symbols:

- A: absorbance.
- **E**: molar absorptivity or absorption coefficient.
- L: length of the Cuvette.
- C: concentration.
- **Io**: the intensity of the incident monochromatic light beam and I the intensity of the emerging light beam.
- **C1:** Concentration of the mother solution.
- **V1:** Volume of the mother solution.
- C2: Concentration of the daughter solution.
- V: Volume of the daughter solution.
- **Q:** Quantity adsorbed per gram of adsorbent (mg/g).
- Co: Initial concentration (mg/L).
- C_e: Equilibrium concentration (mg/L).
- **V:** Volume of the solution (L).
- w: weight of the adsorbate (g).
- **k₁:** Rate constant for pseudo-first-order kinetics (min⁻¹).
- **q**_e: Adsorption quantity at equilibrium (mg/g).
- **q**_t: Adsorption quantity at time t (mg/g).
- **K**₂: Second-order rate constant.

- **Qmax**: Maximum adsorption capacity.
- R²: Correlation coefficient, which indicates the goodness of fit for each model.
- **K**: Thermodynamic equilibrium constant.
- T(K): Temperature.
- **R**: Universal gas constant (8.32 J mol⁻¹K⁻¹).
- ΔH^0 : Enthalpy change (kJ mol⁻¹).
- ΔS^0 : Entropy change (J mol⁻¹ K⁻¹).
- ΔG^0 : Gibbs free energy (kJ mol⁻¹).
- **Tc** (°**C**): Carbonization temperature.
- **tc** (**h**): Carbonization time.
- **TA** (°**C**): Activation temperature.
- ta (h): Activation time.
- Vt (cm³/g): Total pore volume.
- Vmic (cm³/g): Micropore volume.
- **SBET** (m²/g): BET surface area.
- **Y** (%): Yield
- IR (g/g): Iodine number or iodine retention.

Tables list

Number	Title	Page number		
	Chapitre I			
Table I-1	Differences between physical and chemical adsorption	6		
Table I-2	Four stages of the carbonization process	17		
Table I-3	Physical activation of precursors for the production of ACs	19		
Table I-4	Chemical activations of precursors for the production of ACs	20		
Table I-5	Physiochemical activation conditions of precursors for the	22		
Table 1-3	production of ACs	44		
	Chapitre II			
Table II-1	Characteristics of Methylene Blue	36		
Table II-2	Characteristics of methyl orange	37		
Table II-3	Absorbance value	39		
	Chapitre III			
Table III.1:	Parameter values of the two kinetic models	46		
Table III.2	Adsorption modeling by the Langmuir and Freundlich models of	54		
1 abic 111.2	BM	54		
Table III.3	Adsorption modeling by the Langmuir and Freundlich models of	55		
14510 111.5	MO			
Table III.4	Thermodynamic parameters of the adsorption of BM and MO on	57		
1 avie 111.4	activated carbon	31		

Figures list

Number	Title	Page number					
Chapitre I							
Figure I-1	Physical and chemical adsorption	5					
Figure I-2	The Giles Classification of adsorption isotherm	11					
Figure I-3	The IUPAC Classification of Adsorption Isotherms	12					
Figure I-4	Methods of the activation processes	16					
Figure I-5	Biomass is thermochemically converted into gases, charcoal, and bio-oil	17					
Figure I-6	Schematic diagram of AC preparation from biomass by Microwave (MW)	24					
	Chapitre II						
Figure II-1	Diagram of the AC preparation protocol	38					
Figure II-2	Calibration curve of Methyl Orange	40					
Figure II-3	Calibration curve of Methylene Blue	41					
	Chapitre III						
Figure III.1	FTIR spectra of activated carbon	42					
Figure III.2	Kinetic adsorption curve of BM and MO	44					
Figure III.3	Kinetic modeling of BM and MO adsorption on activated carbon	46					
Figure III.4	Adsorption isotherm of BM on activated carbon	48					
Figure III.5	Adsorption isotherm of MO on activated carbon	49					
Figure III.6	the impact of initial dye (BM) concentration on adsorption capacity and removal percentage at 50°C	50					
Figure III.7	the impact of initial dye (MO) concentration on adsorption capacity and removal percentage at 50°C	51					
Figure III.8	Effect of temperature on the adsorption of BM and MO (C0=400m/g; t=120min)	52					
Figure III.9	Isothermal modeling of the adsorption of MO on activated carbon.	53					
Figure III.10	Isothermal modeling of the adsorption of BM on activated carbon.	54					
Figure III.11	The thermodynamic curves of the BM and MO	56					

Summary

•	• 4	•			•		
	AST.	OT.	ลท	brev	กเล	tาก	ns:

List of symbols:	
------------------	--

Tables list

Figures list

Chapte	r I		1
I.1.	Wa	ter pollution:	2
I. 1	l.1.	Types of pollutants :	2
I. 1	1.2.	the effects of water pollution	3
I. 1	1.3.	Common methods for treating polluted	4
I.2.	adso	orption	4
I. 2	2.1.	Definition	4
I.2	2.2.	Types of adsorption	4
I.2	2.3.	Mechanism of adsorption	6
I. 2	2.4.	The factors that influence the adsorption	7
I.2	2.5.	Adsorption capacity	8
I.2	2.6.	Kinetic Adsorption:	8
I.2	2.7.	Adsorption Isotherm	10
I.2	2.8.	Classification by I.U.P.A.C.	11
I.2	2.9.	Linear isotherm models	12
I.2	2.10.	Adsorption Thermodynamics	14
I.2	2.11.	Advanced adsorbent materials	14
I.3.	acti	vated carbon	15
I.3	3.1.	Definition	15
I.3	3.2.	Preparation of activated carbon	15
I.3	3.3.	Applications of activated carbon	24
Chapter	r II		33
II.1.	Intr	oduction	34
II.2.	Mat	erial used	34
II.3.	Equ	ipment	34
II.4.	Chai	acterization methods	35
II.5.	Used	chemical products	35
II.6		ration Curve	
		rimental Protocol	
	•		
		dsorbents	
- 11.	. 1 . 2	TEDALALION OF SLOCK CHIOLIEF ESONILIONS OF THE GVES MICE AND PART	

Cnapter III	41
III.1. Introduction	42
III.2. Characterization of Activated Carbon	42
III.2.1. FTIR analysis	42
III.3. Kinetics of the adsorption of BM and MO dyes on activated carbon	43
III.3.1. Kinetic study protocol	43
III.3.2 Effect of contact time	44
III.4. Modeling the adsorption kinetics of BM and MO dyes on activated carbon	45
III.5 Adsorption isotherm	47
III.5.1 Protocol of the isothermal study	47
III.5.2 Effect of Initial Concentration	49
III.5.3 Effect of temperature	51
III.6 Modeling of the adsorption isotherm	52
III.7 Thermodynamic Study	55
General conclusion	57
References:	59

General introduction

General introduction

Water is the source of all life on Earth, a critical component for human health, environmental

survival, and global economic function. However, contamination from industrial, agricultural, and

home activities is putting water quality at risk. Poor water quality has become a significant global

issue, affecting not just humans but also aquatic plants and fauna.

Colored wastewater having high levels of hazardous chemicals is currently a big concern. Their

presence in effluents poses a risk to living beings. Indeed, the water sector is dealing with major

issues, such as qualitative and quantitative degradation of water resources. These discharges must

therefore be treated before they are dumped into the sewerage system.

There are several water treatment processes, each tailored to certain types of pollutants and

environmental conditions. The most frequent procedures include filtration, disinfection, chemical

precipitation, adsorption, ion exchange, and reverse osmosis.

This paper makes a modest contribution to studies on the elimination of two organic dyes, methylene

blue and methyl orange, via adsorption on activated carbon.

Adsorption kinetics and isotherms were employed to determine the removal mechanisms for these

colors. The kinetic tests were carried out in a stirred beaker reactor after modifying parameters such

as contact time, initial dye concentration, and temperature.

Our manuscript is structured as follows:

In the first section of this thesis, we present a bibliographic summary containing key data on:

Chapter I: Generalities about water pollution, adsorption and activated carbon.

The second part Experimental part carried out on:

Chapter II: Materials and Methods.

Chapter III: Results and Discussion

1

Part I Bibliographical study

Chapter I

Generalities about water pollution, adsorption and activated carbon

I.1. Water pollution:

Water pollution occurs when dangerous substances, usually chemicals or microbes, pollute a stream, river, lake, ocean, aquifer, or other body of water, reducing its quality and making it poisonous to humans or the environment.

The prevalent problem of water contamination endangers human health. Every year, unsafe water kills more people than war and all other types of violence combined. Meanwhile, our drinking water resources are scarce. Less than 1% of the world's freshwater is truly available to humans. Without action, the issues will only worsen by 2050, when worldwide demand for freshwater is anticipated to be one-third more than it is currently. Water is particularly prone to pollution. Water, commonly referred to as a "universal solvent," has the ability to dissolve more chemicals than any other liquid on Earth. It's why we have Kool-Aid and bright blue waterfalls. It also explains why water is so easily polluted. Toxic compounds from farms, towns, and factories quickly dissolve and combine with it, resulting in water contamination[1].

The following are a few of the main categories of water pollutants found worldwide:

I.1.1. Types of pollutants:

I.1.1.1. Chemical Pollutants:

Water quality across the world is under risk due to chemical pollution from mining, urbanization, industry, and agriculture. Runoff, precipitation, and dry deposition are additional ways that air pollutants from these activities might get into bodies of water and turn into water pollutants. While many chemical pollutants have long-term health impacts that are poorly understood, some have substantial and well-known health effects.

There are dissolved compounds in all natural water, some of which are vital nutrients for humans and others of which may be hazardous to their health. A water pollutant's concentration is typically expressed in extremely tiny numbers, such parts per million (ppm) or even parts per billion[2].

I.1.1.2. Organic Pollutants:

Herbicides and pesticides, medications, fuel (including oil spills), industrial solvents and cleansers, and synthetic hormones linked to pharmaceuticals are examples of organic pollutants. Endocrine disruption is a potential effect of these artificial hormones. Many are organic pollutants that stay in the environment for a long time, can be hazardous, and biomagnify via the food chain. The pesticide, the herbicide by-product dioxin, and the liquid insulator polychlorinated biphenyls used in electric transformers are all considered persistent organic pollutants[3].

I.1.1.3. Inorganic Pollutants:

Comprise radioactive isotopes (such as cesium, iodine, uranium, and radon gas) emitted by mining or nuclear accidents, heavy metals, chloride (Cl⁻), and nutrients such nitrate (NO₃⁻) and phosphate (PO₄³⁻).

Although they can come from geologic materials like as phosphorus-rich rock, fertilizer and human and animal waste are the most common sources of nutrients. Nitrogen and phosphorus, which are necessary for the development of microorganisms, are concentrated in untreated sewage and agricultural runoff. Surface water nutrients like phosphate and nitrate can encourage the growth of microorganisms like cyanobacteria, or blue-green algae, which then create toxins and deplete dissolved oxygen (O₂). As previously mentioned in Biogeochemical Cycles, Threats to Biodiversity, and Industrial Agriculture, this process is referred to as eutrophication[4].

I.1.2. the effects of water pollution

I.1.2.1. On human health

Certain water contaminants, including pesticides and industrial chemicals, have been linked to neurological and psychological diseases such as mood swings, sadness, cognitive decline, and anxiety, affecting both men and women. Water pollution has also been linked to bodily problems such diarrhea, skin infections, malnutrition, and cancer. Exposure to particular pollutants may cause early menopause and vasomotor symptoms, increase the risk of cardiovascular disease, and impair bone density[5].

I.1.2.2. On the environment

When water pollution generates an algal bloom in a lake or marine environment, the proliferation of newly supplied nutrients promotes plant and algae development, lowering oxygen levels in the water. This lack of oxygen, known as eutrophication, suffocates plants and animals and can result in "dead zones," in which waters are completely devoid of life. In certain situations, these hazardous algal blooms can create neurotoxins that kill animals, including whales and sea turtles. Chemicals and heavy metals found in industrial and municipal effluent harm rivers. These toxins are hazardous to aquatic life, typically shortening an organism's life span and limiting its capacity to reproduce and move up the food chain as predators consume prey. This is how tuna and other large fish amass high levels of po isons like mercury[6].

I.1.2.3. On economic

producing rashes and other diseases, while also reducing tourism earnings for famous lake sites due to their unsightly appearance and odors[4].

I.1.3. Common methods for treating polluted

There are several treatment methods for removing harmful components from wastewater. These methods include adsorption, membrane separation, electric, chemical, and photocatalytic separation[7]. The most relevant and effective method for removing trace elements from wastewater is determined by a variety of parameters, including ion concentration, removal efficiency, and economic feasibility[8].

Among all methods, Adsorption is the most ensuring approach for separating trace element ions from wastewater because of its high removal effectiveness, technical maturity, broad applicability, cost efficiency, easy operating conditions, environmental friendliness, and low reusability costs. Adsorption can be thought of as a surface phenomenon in which ions, molecules, or atoms of gas, liquid, or **dissolved** solid migrate from a gas or liquid phase to a solid or liquid-solid phase, forming a mono or multi-layer by sticking to the adsorbent's active sites[9]. Thus, adsorption takes place at the solid-liquid interface, where solutes are held on the solid surface. An efficient adsorbent should possess several critical qualities, including high adsorption capacity, rapid adsorption rate, separation recovery, and high selectivity for diverse elements[10]. on this research We will focus on Adsorption Due to its importance, we will take a closer about it and about its types ...etc.

I.2. adsorption

I.2.1. Definition

Adsorption is a surface process that defines the interaction of two different phases that results in the formation of an interface layer by the transfer of a molecule from a fluid bulk (liquid or gas) to a solid surface, In a solid-gas or solid-liquid system, this interface is the solid's surface. Adsorbable molecules in the fluid phase are adsorptive or sorptive, adsorbed molecules are called adsorbate or sorbate, and the solid substance is named adsorbent or sorbent[11].

I.2.2. Types of adsorption

Both physical and chemical forces contribute to solvent adsorption from the solvent. Physical forces include van der Waals and electrostatic forces. Chemical forces arise from short inter-union rates and

the production of internal compounds, such as symbiotic and hydrogen bonds. There are two forms of adsorption:

I.2.2.1. Physical adsorption

Physisorption has weak van der Waals forces, which would lead to low adsorption enthalpies, which are between 5 and 40 kJ/mol. The process is generally reversible and happens at very low temperatures, and it could also occur between multiple layers in the adsorbent material. and there is no changes of chemical structure for both substrate and sorbent [12].

I.2.2.2. Chemical adsorption

the process of chemisorption is based on the formation of strong chemical bonds between the adsorbate and the surface of the adsorbent, by rearrangement of electron density between the adsorbent and substrate, the nature of this bond is ionic bond or covalent bond, and these are known to have higher enthalpies ranging between 40 and 800 kJ/mol, Chemisorption is also irreversible, and these are favored at higher temperatures, which also require higher activation energy[12].

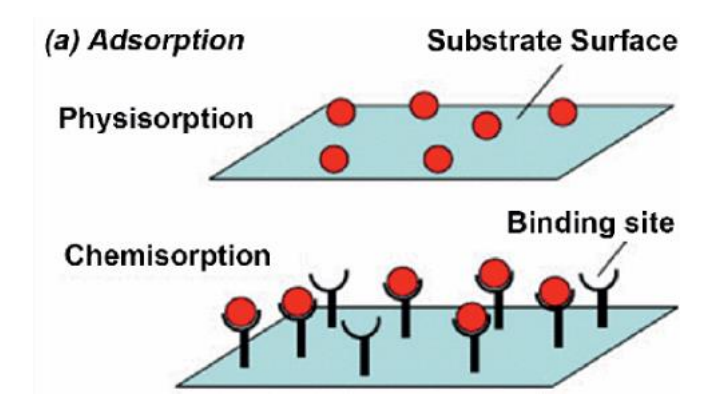


Figure I-1: Physical and chemical adsorption[13].

Table I-1: Differences between physical and chemical adsorption[9].

Criteria	Physical Adsorption	Chemical Adsorption		
Specificity	Non-specific.	Highly-specific		
Nature of adsorption	Depend on nature of	Depend on nature of		
Nature of ausorption	adsorbent.	adsorbent.		
Reversibility	Reversible process.	Mainly irreversible		
		Higher than physical		
Enthalpy	Low (20-40 kJ/mol).	adsorption (40-300		
		kJ/mol).		
Activation energy	Does not require high	Require high activation		
Activation energy	activation energy.	energy.		
Layer of adsorption of		Mono layer.		
interfacial region	Multi layers.			
(saturation)				
	Week Van der Waals,	Strong ionic bond, or		
	London forces, and dipole-	covalent bond formed		
	dipole attraction This	between substrate and		
Randing	attraction has longer range	adsorbent, there is a		
Bonding	than chemical type, and	chemical composition		
	there is no chemical	change. This attraction has		
	composition change for	shorter range than the		
	substrate.	physical type.		

I.2.3. Mechanism of adsorption

The absorption mechanism is divided into four steps:

- The first step (external diffusion) involves the movement of liquid molecules from the external phase to the liquid phase associated with solid particles by diffusion and convection.
- The second stage (internal diffusion) involves transferring the solution through the liquid layer to the adsorbent's external surface.
- In the third step, the adsorbate diffuses into the adsorbent particle due to the concentration gradient.
- The fourth step involves adsorption in a microspore[14].

I.2.4. The factors that influence the adsorption

Factors affecting adsorption include pH, starting adsorbate concentration, contact time, adsorbent dosage, size, temperature, and agitation speed. Optimizing the process parameters is crucial for maximizing percentage removal, and adsorption capacity

I.2.4.1. Effect of pH

The pH parameter is crucial in studying adsorption because it affects the electrostatic charge of ionized adsorbates. The rate of adsorption depends on the medium pH and does not follow a specific pattern. At low pH, anionic molecules have higher adsorption capability than cationic molecules[15]. As the pH of the medium increases, electrostatic repulsion between the positively charged adsorbate and the adsorbent surface decreases, leading to an increase in surface charge density[16].

I.2.4.2. Effect of Contact Time:

Equilibrium research indicates that adsorption capacity rises with contact time until a threshold is reached when further contact time does not increase adsorbate uptake due to saturation. The amount of adsorbate desorbing from the adsorbent in solution and adsorbed onto the adsorbent is in dynamic equilibrium. The equilibrium time determines the adsorbent's maximum adsorption capacity under operational conditions[17]. Adsorption performance greatly depends on the contact period between adsorbents and adsorbates.

I.2.4.3. Effect of Initial Adsorbate Concentration

elevating the initial adsorbate concentration leads to higher percentage removal and lower adsorption capacity. To test the impact of initial adsorbate concentrations, a solution is prepared at varying concentrations with fixed pH, temperature, and contact duration parameters. The effect of initial adsorbate concentrations on the interaction between adsorbates and adsorbents is studied using isothermal models[18].

I.2.4.4. Effect of the Adsorbent Dosage

Adsorption capacity is determined as the amount of adsorbate extracted per mass of adsorbent used. Adsorption rates increase with increasing adsorbent dose due to the increased number of sorption sites on the adsorbent's surface. To investigate the impact of adsorbent dosage on the adsorption process, trials are conducted using varying adsorbent masses at a fixed starting adsorbate concentration and equilibrium time[19].

I.2.4.5. Effect of Temperature

Temperature affects adsorption via influencing bond characteristics between adsorbate sites and adsorbents, as well as adsorbate solubility in the medium. Adsorption rises for both strong and weak connections at low temperatures, while weak forces diminish[20].

I.2.4.6. Effect of Adsorbent Size

As particle diameter decreases, adsorption rate rises due to increased surface area. Smaller particle sizes reduce the restriction of adsorbate penetration into the adsorbent because of internal difusion and mass transfer. This leads to faster equilibrium and maximum adsorption capacity[21].

I.2.4.7. Effect of Mixing Speed

The importance of agitation's speed in the adsorption process is significant. The observations demonstrate that the intensity of agitation's speed can have a significant impact on the amount adsorbed[22].

I.2.5. Adsorption capacity

Adsorption investigations are often carried out in batches. Equations (1)-(3) compute the adsorption capacity (q_t and q_e) and removal efficiency (RE,%) of adsorbate-based compounds[23].

$$q_t = \frac{(C_0 - C_t)v}{w} \dots (1)$$

$$q_e = \frac{(C_0 - C_e)v}{w}$$
(2)

$$RE = \frac{(C_0 - C_e)}{C_0} \times 100....(3)$$

where C_0 (mg/L), C_t (mg/L), and C_e (mg/L) are the adsorbate concentrations at the beginning time, time t, and equilibrium time, respectively; W (g) is the mass of dried adsorbent; and V (L) is the volume of the aqueous phase.

I.2.6. Kinetic Adsorption:

Adsorption kinetics describes the rate of retention or release of a sorbate from aqueous solution to solid-phase interface. In adsorption, linear or non-linear analysis of the kinetics is applied. The goodness of fit index is applied to determine the model that best describe the process[24].

Previous research described the kinetic adsorption mechanism in two phases. The first step presupposes that the adsorbate transfers from the bulk solution to the adsorbent's surface[25]. The second stage diffuses the adsorbate and organizes it within the sorbent pores. The rate-limiting stage of adsorption reveals the underlying mechanism[26].

I.2.6.1. Pseudo-first-order reaction kinetics

The adsorption rate constant assumes first-order reaction kinetics.

[25]
$$\frac{dq_t}{dt} = k_1(q_e - q_t)$$
(1)

The equation for first-order adsorption includes k_1 as the adsorption rate constant, q_t as the quantity adsorbed at time t (mg/g), and q_e as the amount adsorbed at saturation (mg/g).

The integration of equation (1) yields the following expression:

$$ln(q_e - q_t) = -k_1 * t + c_1....$$
 (2)

Where C_1 is the integration constant for the first order reaction kinetic, Integrating Equation (2) with the boundary conditions t = 0 to t = t and t = t plateaus, yields the following expression:

$$ln (q_e - q_t) = ln q_e - k_1 t$$
(3)

The slope and intercept of the linear plot of $\ln (q_e - q_t)$ versus t yield the values of k_1 and $\ln q_e$, respectively. Comparing the q_e values derived from the plot intercepts to those acquired experimentally demonstrates that the adsorption process is a first-order kinetic reaction.

I.2.6.2. Pseudo-Second-Order Reaction Kinetic

If the adsorption process follows the pseudo-second-order reaction kinetic, it may be modified using the following mathematical formulae[25].

$$\frac{dq_t}{dt} = k_2 (q_e - q_t)^2(4)$$

The equation for second-order adsorption is as follows: k_2 is the adsorption rate constant, q_t is the quantity of substrate adsorbed at time t, and q_e is the amount of substrate adsorbed at saturation (mg/g).

If equation (4) is integrated, the following expression is obtained:

$$(1/q_e - q_t) = k_2 * t + c_2 \dots (5)$$

In this equation, k_2 is the second order reaction constant (g mg⁻¹ min⁻¹), while q_e and q_t represent the quantity of metal ions adsorbed per unit weight at equilibrium and time t, respectively. Integrating equation (5) with the boundary conditions t = 0 to t = t and t = 0 to t

$$\frac{t}{q_t} = \frac{1}{k_2 \, q_e^2} + \frac{t}{q_e} \tag{6}$$

To compute q_e and k_2 are calculated by plotting of t/q_t vs. t, which yields a straight line. Experimental qe values are then compared to the calculated value.

I.2.7. Adsorption Isotherm

Adsorption isotherms explain the pathway of a substrate's interaction with the bulk solution to the surface of the adsorbate. It describes the relationship between the quantity of substrate adsorbed per unit mass of adsorbent and the substrate concentration or pressure in the bulk solution at a constant temperature [25].

Temperature plays a crucial part in determining the adsorption process between sorbent and adsorbate. It also determines whether temperature has a positive or negative impact on the process. Adsorption isotherms were divided by Giles into four categories: L (Langmuir type), H (high affinity), S (cooperative), and C (constant partition) (Figure 2). The categorization is based on the bottom section of the curve when the adsorbate solution is very dilute.

S-type isotherm refers to cooperative adsorption, where adsorbate-adsorbate interactions are greater than adsorbate-adsorbent interactions. Adsorbate molecules cluster at the surface due to stronger interactions with one another (Figure 2)[27].

The L-type isotherm indicates chemisorption, as the adsorbate has a high affinity for the adsorbent. This isotherm occurs when the contact between adsorbate and solution is weaker than that between adsorbate and adsorbent (Figure 2)[27].

The H-type isotherm is an extension of the L-type, indicating a high affinity of the adsorbate for the adsorbent. In dilute solutions, the adsorbate is practically fully adsorbed (Figure 2)[27].

The C-type isotherm shows a consistent proportionate affinity between adsorbate molecules and adsorbent at low concentrations (Figure 2)[27].

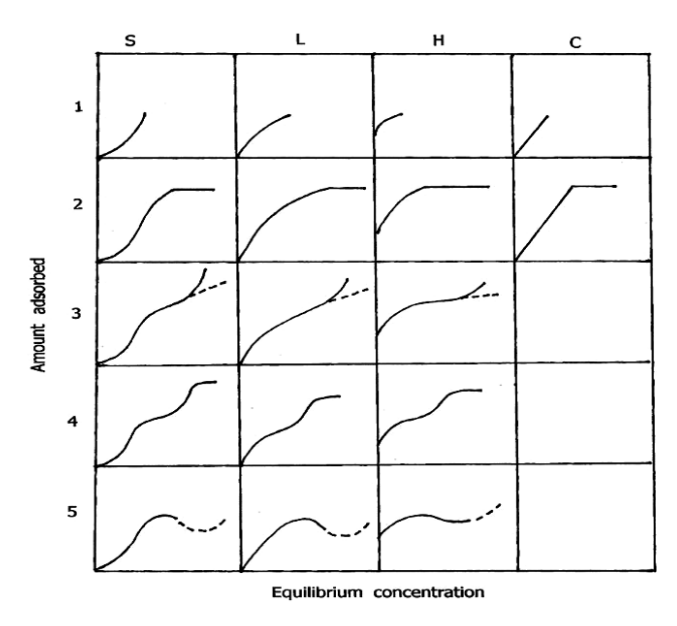


Figure I-2: The Giles Classification of adsorption isotherm[27].

I.2.8. Classification by I.U.P.A.C.

The International Union of Pure and Applied Chemistry (IUPAC) categorizes adsorption isotherm models into six kinds (I, II, III, IV, V, and VI) based on their shape (figure 3)[28]. The Type I model is reversible and concave along the relative pressure axis, Examples of this type include molecular zeolites and activated carbon[28]. The regular type II isotherm model can be developed from a non-porous adsorbent, One example is the adsorption of nitrogen on silica gel[29]. The reversible type III isotherm model is convex on the pressure axis, and a common example is water vapour adsorption on nonporous carbon[30]. Type IV isotherms have hysteresis loops caused by capillary condensation in mesopores, which limits uptake at high pressures. The type IV isotherm model describes the adsorption of humid air or water on activated carbon[31]. The type V isotherm model is similar to the type III model due to their poor adsorbent-adsorbate interaction[32]. The model is unusual but can be found in some porous adsorbents. A common example is water adsorption on a carbon molecular sieve or activated carbon fiber[31]. The type VI isotherm model involves multilayer, sequential adsorption on a nonporous surface. This concept applies to the adsorption of inert gases on planer graphite surfaces[33].

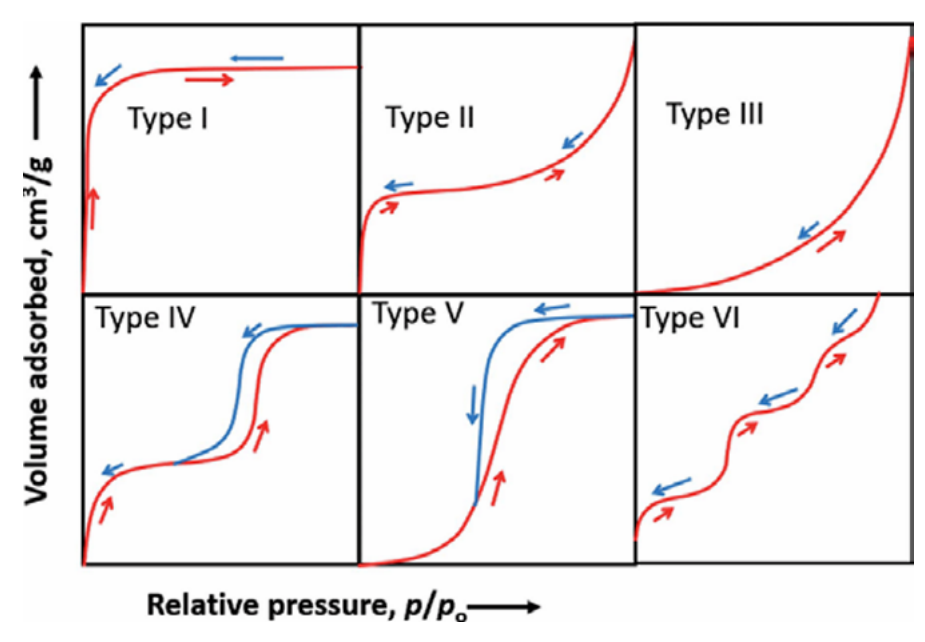


Figure I-3: The IUPAC Classification of Adsorption Isotherms[28].

I.2.9. Linear isotherm models

I.2.9.1. Langmuir Adsorption Isotherm

The Langmuir isotherm is the simplest isotherm model, developed in 1916 from research into gas adsorption by materials. The single adhesion layer on a homogeneous surface [34] reduces the attraction between adsorbed molecules and non-adsorbed analytes in the bulk solution as they move away from the adsorbate surface.

The Langmuir equation implies a monolayer adsorption with no attraction between molecules on the adsorbate surface. This assumption has limitations. This approach applies to gas systems with low concentrations or pressures.

The Langmuir isotherm is defined using the following mathematical equations:

$$q_e = q_m * k * C_e / (1 + kC_e)$$
....(9)

Equation (9) can be written in the following linear form (I): where q_e is the equilibrium amount of solute adsorbed per unit mass of adsorbent (mg/g), Ce is the equilibrium concentration of solute (mg/L), q_m is the adsorption capacity of the monolayer (mg/g), and K_L is the Langmuir constant related to the energy and affinity of binding sites of adsorption: $k_d = \frac{C_e}{q_e}$

$$\frac{q_e}{C_e} = q_m k_L - k_L q_e \qquad (10)$$

Langmuir's other linear forms may be obtained by taking the inverse of equation (9), yielding linear form II.

$$\frac{1}{q_e} = (1/(q_m * k_L)) * (1/C_e) + 1/q_m....(11)$$

Alternatively, to obtain the linear form (III), multiply equation (11) by Ce.

$$\frac{C_e}{q_e} = 1/(q_m \, \mathbf{k}_L) + (1/q_m) * C_e$$
 (12)

The slope and intercept of the Langmuir equation's linear versions may be used to calculate q_m and k_L values. The Langmuir isotherm model has a dimensionless constant known as the equilibrium parameter RL, as stated in [35]: $R_L = \frac{1}{1 + K_L C_0}$

The value of R_L reflects the isotherm's behavior as unfavorable adsorption ($R_L > 1$), linear adsorption ($R_L = 1$), no adsorption ($R_L = 0$), or favorable adsorption ($0 < R_L < 1$), with Co being the greatest starting concentration.

I.2.9.2. Freundlich Adsorption Isotherm

Freundlich isotherm, a subset of Langmuir, models multi-layer adsorption on heterogeneous surfaces and may be described by the equations below[36].

$$q_e = k_F C_e^{\beta} = k_F C_e^{1/n}$$
....(13)

In this equation, q_e represents the equilibrium quantity adsorbed per unit mass of adsorbent (mg/g), Ce represents the adsorbate's equilibrium concentration in solution (mg/L), K_F is the Freundlich isotherm constant, and n represents the adsorption intensity.

The logarithmic linear version of the Freundlich equation is as follows:

$$\log q_e = \log(K_F) + (1/n)(\log C_e)....(14)$$

I.2.9.3. Dubinin- Radushkevich (D-R) Isotherm

Langmuir and Freundlich isotherms are basic models that describe adsorption's physical and chemical properties through layer-by-layer surface covering. The Dubinin-Radushkevich (D-R) isotherm is a typical model for describing sorption isotherms for single substrate systems. The D-R isotherm is similar to the Langmuir isotherm, except it excludes homogenous surfaces and constant adsorption potentials. It proposes an adsorption mechanism that involves pore-filling of the sorbent rather than layer-by-layer surface covering.

The liner D-R isotherm is stated as follows:

$$ln q_e = ln q_{max} - \beta \varepsilon^2 \dots (15)$$

In this equation, q_e is the quantity of substrate removed per unit adsorbate mass, q_m represents the D-R adsorption capacity (mg/g), β is an adsorption energy constant (mol² kJ²), and ϵ represents the Polanyi potential.

Equation (15) calculates the Polanyi potential (ε) as follows:

$$\varepsilon = R T ln (1+1/C_{\rho})$$
(16)

Where R is the gas constant (kJ K⁻¹ mol⁻¹), and T is the temperature (K).

The primary energy of adsorption (E) is computed using the following formula:

$$E = (2 \beta)^{-0.5}$$
....(17)

E is the free energy change necessary to transport one mole of ions from solution to a solid surface, providing information on the physical and chemical properties of adsorption [25].

I.2.10. Adsorption Thermodynamics

The following equations were used to determine thermodynamic parameters, including free energy (ΔG^{o}) , enthalpy change (ΔH^{o}) , and entropy change (ΔS^{o}) :

$$\Delta G^0 = -R T \ln k_d \dots (18)$$

$$\ln k_d = (\Delta S^0 / R) - (\Delta H^0 / RT)$$
(19)

In equation (20), R represents the gas constant (8.3145 J.mol⁻¹ K⁻¹), T is the temperature in Kelvin, and k_d is the thermodynamic distribution coefficient:

$$k_d = \frac{q_e}{c_e} \tag{20}$$

To determine ΔH^0 and ΔS^0 , use the slope and intercept of $\ln k_d$'s linear fluctuation with reciprocal temperature. The $\ln k_d$ was derived using the intercept of $\ln (q_e/C_e)$ versus q_e [37].

I.2.11. Advanced adsorbent materials

Adsorbent materials are essential in both the adoption process and in applications categorized as emerging like Metal-Organic frameworks, Covalent-organic frameworks, Graphene-based materials,

and classic materials like Activated carbon, Zeolites, Silica gels[38], on thi research We will focus on activated carbon.

I.3. activated carbon

I.3.1. Definition

Activated carbon is a very adaptable porous adsorbent that is utilized in a wide range of separation and purification procedures for both gas and liquid phase systems. Activated carbon is an amorphous carbon-based material with a high porosity, large surface area, microporous structure, high adsorption capacity, and surface reactivity. Activated carbon may be made from a range of low-cost cellulosic materials, including wood, rice straw, nutshell, maize hull, coconut shell, oil-palm shell, longan seed, bamboo, and peach stone, as well as carbonaceous sources such bituminous coal, lignite, and peat. This study examines the efficacy of several types of activation procedures for activated carbon derived from biomass. The adsorption capability of toxins and pollutants from water and air has been thoroughly documented in order to get pure water and clean air.

I.3.2. Preparation of activated carbon

Activated carbon is prepared in two fundamental processes. The first one is carbonization, and the second is activation. To generate biochar[39], carbonization is carried out via pyrolysis/gasification at a higher temperature in an inert environment[40]. At this point, the carbon content of the carbonaceous material was determined by eliminating the volatile components by thermal decomposition. The temperature, heating rate, nitrogen gas flow rate, and residence duration are important characteristics in this step. Because the obtained biochar has limited adsorption capacity, an activating step is required to increase the pore volume, pore diameter, and surface area[41]. In the activation process, initially, the disordered carbon was removed, exposing the lignin to the activating chemicals. Depending on the type of activation, activation can be a process that occurs before or after carbonization to remove deposited tarry substances in biochar, which can help to enhance the porosity and provide high surface areas for the Activated Carbons (ACs)[42]. The primary activation process that produced the activated carbon from biomass is depicted in Figure I-4. Initially, the disorganized carbon was removed, exposing the lignin to the activating agents and developing the microporous structure. Lastly, the existing pores are widened to a large size by burning the walls between the pores, which increases the intermediate pores and macro-porosity and decreases the volume of micro-pores.

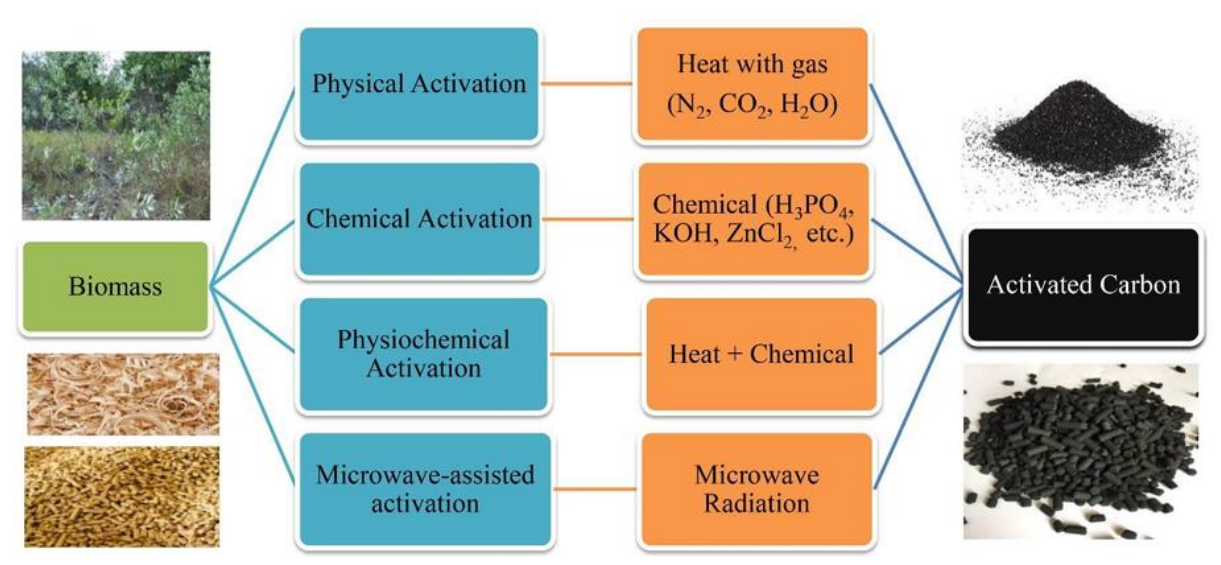


Figure I-4: Methods of the activation processes.

The process of activating carbon begins with the removal of tarry materials, which helps the activating chemical react with biochar later on and removes tar deposits that clog pores[43]. An activating agent is then used to oxidize the carbon particles in biochar after they have been burned. The two most crucial factors to consider for the creation of porous structures are activation temperature and time. According to reports, these characteristics are inversely connected with the yield of AC, yet they correspond to the pore volume. The carbonization of biomass is the first step in preparing AC, and it is important to regulate and limit the high temperature because high-temperature activation may result in the development of undesirable chemicals during the material's thermal breakdown[44].

I.3.2.1. Carbonization / pyrolysis

The thermal breakdown of raw materials in a furnace under N2 purge in an inert atmosphere is known as carbonization or pyrolysis. This process removes volatile non-carbon species like nitrogen, oxygen, and hydrogen and increases the fixed carbon content to create biochar[40]. Narrow pore structures of precursors begin to form during the devolatilization process, causing tarry compounds to be deposited as the temperature rises[45]. In certain instances, this deposition may result in the collision of certain tarry materials and the collapse of pore walls, which lead to carbon deposition and hydrocracking[46]. A four-stage synopsis of the carbonization process is presented in Table I-2.

Table I-2: Four stages of the carbonization process[47]

Stage	Temp (°C)	Type of reaction	Process
1	≤200	Endothermic	Initial drying of raw materials to remove moisture
2	170–300	Endothermic	Pre-carbonization phase: To produce some pyroligneous liquids (acetic acid and methanol) and light tars and non-condensable gases (CO and CO ₂)
3	250–300	Exothermic	Bulk removal of pyroligneous liquids and light tars produced in stage 2 – producing biochar
4	>300	_	Drive off volatile and non-carbon species to enhance fixed carbon content of biochar

A careful choice of parameters is crucial since the carbonization parameters have a big impact on the process and have a big impact on the quality of the finished products[48]. As seen in Figure I-5, the carbonization residency or holding time is the most crucial factor, followed by the amount of inert gas and its flow rate, the heating rate of reactions, and the carbonization temperature, which has the biggest impact on the process. Increases in temperature typically result in the release of more volatile species as well as an increase in the amount of ash and fixed carbon. But doing so lowers the amount of biochar produced[44]. The primary breakdown (de-volatilization) of biomass at high temperatures and the secondary decomposition (cracking) of biochar residue are assumed to be the causes of the yield decline. As a result, higher temperatures yield higher-quality biochar[49].

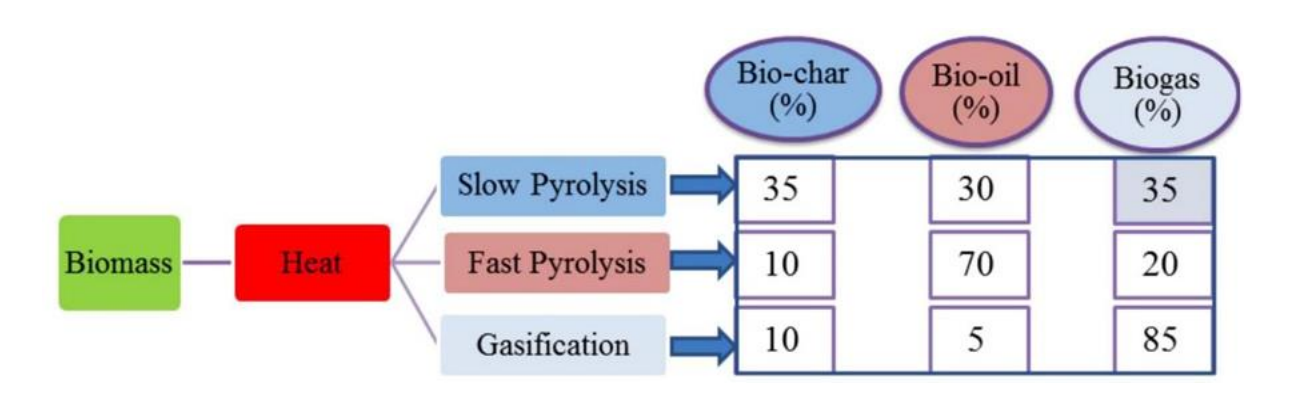


Figure I-5: Biomass is thermochemically converted into gases, charcoal, and bio-oil[50].

I.3.2.2. Physical activation

There are two possible processes for physical activation: one-step and two-step[51]. Physical activation is usually a two-step method. First, dried materials are carbonized at 400–700°C to create biochar. Next, oxidizing gases such as steam, air, CO₂, or their mixes are used to activate the samples at a high temperature of 800-1100°C to cause some burn off[52]. The surface area of carbonization-derived biochar is usually less than 300 m²/g[53]. Tarry chemicals that can be activated are responsible for the pores' reduced surface area and adsorption capacity[43]. When the temperature is maintained between 600 and 800 °C[54], carbonization and activation take place concurrently as a single phase. Like the dual-stage method, the single-stage method carbonizes the dried sample until a certain temperature is reached, but biochar can be heated for an additional amount of time simply by changing the inert gas to an oxidizing gas. Although the processes are comparable, the single-step method is far more practical since it omits the chilling stage following carbonization, which can lower operation time, cost, electrical consumption, and physical labor[53].

In addition to expanding the small pores that have formed on the surface of the biochar, physical activation also creates new pores, increasing the porosity and surface area of the carbonaceous porous structure [44]. However, because of the greater activation temperature and longer activation period, physical activation typically results in a comparatively lower carbon yield and quality of AC than chemical activation [51].

As seen in Table I-3, steam and CO₂ are frequently employed as activating agents in physical activation. Because of the exothermic nature of the reactions, which can result in excessive burning on the internal and external surfaces of the biochar and lower yield[47], air (oxygen) is less desirable as an activation agent. Both steam and CO₂ react with carbon to produce maximum surface areas that can exceed 1000 m²/g and even higher values, as shown in Table I-3, which suggests that they generate comparable maximum BET surface areas. Despite the similarities in the treatments, there are some subtle differences in their mechanism and reaction. According to Rafsanjani et al.[55], water molecules can more readily permeate into the pores of biochar because they are smaller than CO₂, which causes a faster reaction between the carbon and CO₂ and the development of new pores[56]. Steam is said to react with carbon four times more quickly than CO₂ at a temperature close to activation[53]. As a result, AC can quickly reach a large surface area through steam activation[57]. Steam activation encourages the expansion of micropores toward the development of mesopores and macropores from the start of the activation process at a typical heating rate, whereas CO₂ activation places more emphasis on the creation of new pores than the widening of narrow pores. The resulting ACs will have a wider pore distribution thanks to this[44]. Even at a higher

activation rate, the percentage of mesoporous and micro-porous structures for steam activation and CO₂ activation, respectively[53], would increase. In certain situations, CO₂ activation seems to be the better option because it is cleaner, the gas is easier to handle, and its slow reaction rate allows it to control the activation process even at high temperatures up to 800 °C[58].

Table I-3: Physical activation of precursors for the production of ACs[59]

Precursors	Carboni		Activation conditions			Textural properties			
	T _C (°C)	t _c (h)	Activator	T _A (°C)	t _a (h)	V _t (cm ³ /g)	$\begin{array}{c} V_{mic} \\ (cm^3 / g) \end{array}$	$S_{BET} \\ (m^2/g)$	Y (%)
Acacia mangium	_	_	CO_2	500	2.0	0.176	0.126	395.9	_
Acacia mangium	300	0.5	N_2	500	2	_	_	377.18	_
Walnut shell		_	Steam	800	2.5	_	_	1064.2	_
Date pits	_	_	Steam	800	1	_	_	702	_
Rice husk	_	_	Steam	850	1.75	1.09	_	1180	_
Date palm tree fronds	_	_	Steam	577	0.5	0.4382	_	1094	_
Industrial pretreated cork	_	_	Steam	800	1	_	0.28	750	_
Camellia oleifera	_	_	Steam	820	_	1.17	_	1076	_
Oil palm EFB	_	_	Steam	-	_	0.341	_	720	_
Cypress sawdust + PKS ash	600	_	Steam	_	_	_	_	1668.1	_

I.3.2.3. Chemical activation:

Chemical activation can occur in one or two stages. The carbonization technique is the only difference between the two[44]. Carbonization does not occur in the single-stage procedure, and the dried sample is activated in the main phase by reacting with dehydrating agents such as NaOH, KOH, ZnCl₂, and H₃PO₄[60]. The dual-stage technique involves carbonizing the dried material to generate biochar at temperatures ranging from 400 to 600 °C before chemical activation[51]. Table I-4

presents a summary of chemical activation data. Chemical activation can be applied in three ways: (i) Basic activation, (ii) acidic activation, and (iii) neutral activation.

Table I-4: Chemical activations of precursors for the production of ACs[61]

Precursors	Carbo	onization ditions	Activa	Activation Te conditions			Textural properties			
	T _C (°C)	t _c (h)	Activ ator	T _A (°C	t _a (h)	V _t (cm ³ / g)	V _{mic} (cm ³ /g)	S _{BET} (m ² /g	Y (%)	IR (g/g)
Acacia fumosa seed		I	HCl	450	6	_	_	I	_	_
Acacia mangium	_	I	КОН	500	2	0.015		5.25	_	2:1
Acacia mangium	-	-	CaO	500	2	0.090		65.53	_	2:1
Acacia mangium	500	2	ZnCl ₂	_	_	0.555	0.337	957.4 7	_	0.5:1
Acacia mangium	500	2	H ₃ PO 4	_	_	0.422	0.357	1038. 77	_	0.5:1
Acacia mangium	_	_	H ₃ PO 4	500	0.75	_	_	1767	_	0.4
Acacia Nilotica Sawdust	_	l	H ₃ PO ₄	900	1	_	_	1701	_	1:0.5
Acacia arabica	_	_	H ₃ PO 4	200	0.5	_	_	_	_	2:1
Acacia nilotica	_	_	ZnCl ₂	600	5		_	403	_	
Walnut shell	_	_	КОН	800	3	1.10	_	2259. 4	_	0.5

The observations summarized in Table I-4 show that carbonization and activation settings, activator selection, and impregnation ratio may all influence the textural features and quality of the AC[43]. Depending on the dehydration agent employed, various precursors react differently, resulting in a range of surface areas, pore volumes, and yield[62]. Activating biomass with metal alkaline hydroxides like KOH and NaOH results in ACs with large surface areas, up to 2000 m²/g (Table I-4). However, the use of metal alkaline hydroxides is limited by the kind of precursor. Cao et al[63]. found that metal alkali hydroxides are commonly used in the dual-stage procedure because they function more efficiently with charcoal. Char created by carbonization of precursors comprises a particular amount of holes that allow dehydrating agents to diffuse and react with carbons, producing ACs with large surface areas and porosity over time[44]. Metal alkali hydroxides may have difficulty

entering precursors due to the low porosity of the raw materials[47]. Impregnation alone is inadequate to create porous active carbon, necessitating a two-stage chemical activation. For example, in a study by Isoda et al[64]. using NaOH on rice husk activated surface areas by 280 and 660 m²/g, respectively. It is also stated that biochars are substantially more sensitive to KOH activation, which may assist develop ACs with high-quality surface characteristics[65], Table I-4 shows that the most widely utilized activator is H₃PO₄. This might be owing to the fact that necessary activation is less economically advantageous than acidic activation since it costs more. Acidic activation employing H₃PO₄ as a more cost-effective approach can result in a larger percentage of yields[61]. Increases the overall number of micropores and mesopores, causing considerable variations in the surface area, porosity, and reactivity of the end product[66]. In another work, Arami-Niya et al.[67],[68] investigated the effects of acidic and neutral activation of oil palm shell with H₃PO₄ and ZnCl₂. Both the surface area and pore volume acquired with acidic activation are claimed to be greater than those obtained with neutral activation. The variations in textural qualities were attributed to the rate of activation, which is higher for H3PO4 (8.86% burn-off per hour) and lower for ZnCl₂ (22% burn-off per hour)[68]. Nonetheless, from an environmental standpoint, metal alkali hydroxides and acids are less preferred as activators since they are corrosive, poisonous, dangerous, and have a high risk of triggering an explosion when precautions are necessary[61], As a result, more dependable dehydrating agents, such as K₂CO₃, are utilized instead in single-stage activation to create activated carbons and alleviate the issue of basic and acidic compounds contributing to secondary waste disposal[47],[53]. Chemical activation is a better alternative for activation than physical activation in terms of surface area development, micro-pores, increased carbon yield, and economic feasibility due to lower activation temperature and shorter activation time[61]. However, its shortcoming is that chemical agents remain on char, and a second washing stage is necessary to be completely eliminated [47], followed by physical activation of char (physiochemical activation) [53].

I.3.2.4. Physiochemical activation:

In addition to physical and chemical activation, physiochemical activation allows for simultaneous activation[47]. There are two techniques for manufacturing ACs with physiochemical activation: (i) chemical treatment before to carbonization (pre-carbonization), and (ii) chemical treatment after carbonization[53]. The first method involves carbonizing precursors, impregnating them with biochar, and then thermally treating them with oxidizing gas. The second method involves chemically treating precursors before thermal treatment and physical activation at elevated

temperatures ranging from 600 to 850 °C[53]. Lee et al[69]. said that the order of chemical activation in this process influences the quality and textural features of the resulting ACs.

In the investigations presented in Table I-5, the pre-carbonized sample and post-carbonized char for chemicals were compared in numerous ways. Chemically treated pre-carbonized samples have a surface area of 990 m²/g and a pore volume of 0.42 cm³/g, whereas post- carbonized char has a lower surface area of 680 m²/g and a pore volume of 0.30 cm³/g. The post-carbonized sample's decreased surface area is due to the dehydrating agent's pore- blocking effect[70]. Thus, physical stimulation could be used to clear the barrier. Chowdhury et al.[47] noted that physiochemical activation can be used when a dehydrating agent remains on the surface of biochar after washing, resulting in pore blockage. Hence, an additional physical activation step is required to maximize the porosity of biochar[71].

Table I-5: Physiochemical activation conditions of precursors for the production of ACs[59].

Table 1-3. 11	Carbo	onization								r v Te v Tr
Precursors	con	ditions	condi	tions						
	T _C (°C)	t _c (h)	Activa tor	T _A (°C)	t _a (h)	V _t (cm ³ /g)	V _{mic} (cm ³ /g)	S_{BET} (m^2/g)	Y (%)	IR (g/g)
Oil palm fronds		I	KOH/ CO ₂	-		0.667	_	1237.13	_	-
Rice husk	_	_	KOH/ CO ₂	800	2	1.126	0.805	1836	23	-
Rattan sawdust	700	1	KOH/ CO ₂	750	2	-	-	_	-	_
Kenaf core	400	2	KOH/ CO ₂	_	_	-	-	_	-	_
Peach stones	-	_	H ₃ PO ₄ / CO ₂	_	9	2.0	-	_	-	1: 0.91
Acacia nilotica	_	_	H ₃ PO ₄ / N ₂	250	3	-	-	_	-	-
Date pits	600	_	HNO ₃ / Steam	_	3	0.750	_	950	_	_
Date pits	600	-	H ₃ PO ₄ / Steam	_	3	0.850	_	1100	_	1
Date pits	_	_	KOH/ CO ₂	850	2	0.424	_	763	20	_
Coconut shell	500	3	ZnCl ₂ / Steam	900	0.5	_	_	_	_	_

Several research comparing physiochemical and chemical activation techniques have found that double-step activation yields ACs with varied but superior textural qualities and quality. Arami-Niya et al[72]. reported that ACs generated by physiochemical activation have well- developed and evenly dispersed pore architectures. In another study, surface areas altered between 1035-1653 m²/g and 554-1213 m²/g for H₃PO₄ and CO₂ activation and solitary CO₂ activation, respectively. Even with alone CO₂ activation, the optimum holding duration was 2h longer (7 h) than with double-step activation[68], the surface area of AC produced from solo CO₂ activation was reported to be 632 m²/g, with a pore volume of 0.26 cm³/g[69], Tseng et al[73]. also reported in their work that when carbons are soaked with KOH, only micro-pore structures emerge on their surfaces. Meanwhile, when impregnated carbon is subjected to heat treatment with CO₂ gas for physiochemical activation, the ratio of macropores to mesopores increases, which explains the increase in porosity and mass transfer for enhanced adsorption capability[74].

I.3.2.5. Microwave-assisted activation

Microwave (MW) activation has proven to be a viable alternative to traditional methods of producing activated carbon due to its unique characteristics such as selective, rapid, even, and volumetric heating, indirect interaction between the heating foundation and heated resources, and prompt and precise regulation[75]. The key working restrictions for microwave-supported activation include procedure design, MW radiation strength, activation period, precursor qualities, and MW-chemical interactions[51]. Dipole orientation and ionic transport allow energy to be easily distorted into heat inside the molecules during MW heating, when exposed to a high-frequency voltage[76], particles with induced or permanent dipole moments align in the opposite direction of the applied force. As a result, a considerable temperature gradient moves from the inside of the sample molecule to its cool outside, making it more functional and efficient[77]. MW aided activation is a mix of physical and/or chemical activation that can create higher quality activated carbon through one- or two-step activation methods, as depicted in Figure I-6.

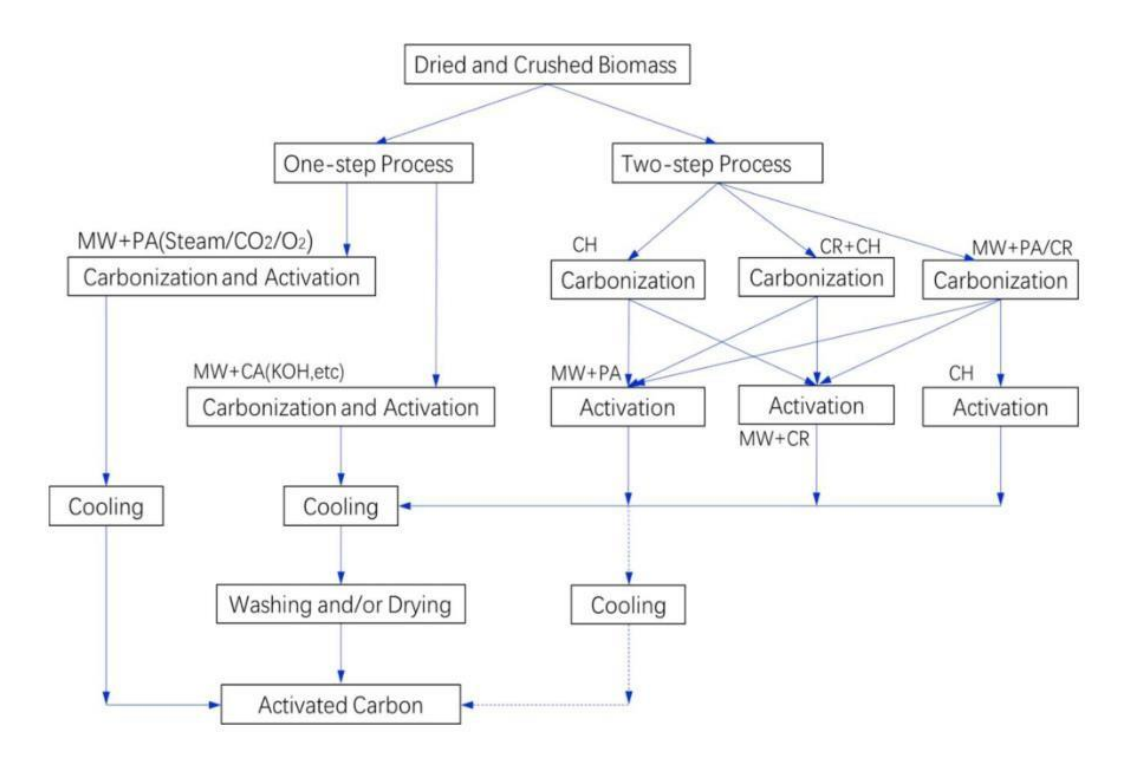


Figure I-6: Schematic diagram of AC preparation from biomass by Microwave (MW)[51]

Carbonization and activation are the two primary processes for one-step microwave activation using a reactor. The benefit of this activation is the ability to obtain AC with a stable configuration through a simple method. Microwave activation is a two-step process that involves carbonizing and activating biochar. The BET surface area in this process is determined by the biomass supplies, pyrolysis temperature, radiation power, operating time, and additives[51]. Microwave activation is a versatile process for extremely controllable components as well as creating ACs with improved pore dispersion and textural properties[78].

I.3.3. Applications of activated carbon

Because of the scarcity of water, AC has become more widely employed in water purification to remove impurities and toxins[57]. According to reports, almost 80% of ACs used worldwide are administered in liquid-phase or aqueous solutions. ACs have been shown to be among the most important and effective adsorbents for organic and inorganic contaminants. The variety of adsorption capacity, surface area, and porous structure of ACs are the primary reasons for their applicability. When carbons come into contact with an aqueous solution, the surface structure in the ACs dissociates or absorbs the ions in the solution, resulting in electric charges. The dissociation or intensity of attraction is determined by the pH of the solution and the surface properties of the adsorbent.

Many studies have lately acknowledged the application of green synthetic nano-composites to remove pollutants and contaminants from water, using nanoparticle loading technology on air conditioners for better adsorption efficiencies and absorption capacities. In this context, tungsten oxide nanoparticles, zero-valent iron nanoparticles, iron oxide nanoparticles, and Ag nanoparticles were loaded onto ACs, which are primarily employed to remove dyes and metal contaminants. The pH of the solution is an important factor in determining the surface charge density as well as whether the surface is positive or anionic. Thus, low pH solutions attract anions, whereas high pH solutions attract cations. Thus, the pH of the solution may be adjusted the absorption of charged inorganic groups. Acidic carbons are more suited to keeping cations, whereas basic carbons are more successful at removing anions[79].

I.3.3.1. Inorganic contaminants found in water

1. Metal pollutant removal:

Metallic pollutants, such as heavy metals and metalloids, are toxic to water, biomagnify in food chains, and are not biodegradable. Their presence is harmful and can accumulate in the human body or living organisms, resulting in long-term health problems and illness[80]. Furthermore, they feature tiny and complicated structures that provide substantial worry since they are difficult to remove. These pollutants are biomagnified in the food chain, and are non-biodegradable. Their presence is harmful and can accumulate in the human body or living organisms, producing long-term health problems and illness. Furthermore, they feature tiny and complicated structures that are of great concern since they are difficult to remove.

The adsorption process on activated carbon is influenced by several factors, including metal ion interaction, pH, surface area, oxygen functionality, and ion size (typically 1.0-1.8 nm) with tapered microporosity. The interactions between the adsorbent and adsorbate are determined by electrostatic, non-electrostatic, and dispersive forces, all of which play a vital part in the adsorption process.

On several types of adsorbents employed to remove metallic contaminants, including their adsorption capabilities and experimental settings. The removal effectiveness of chromium with Acacia mangium AC was 37.16 mg/g, whereas Acacia nilotica Bark AC was 93.1%[71]. Lead is one of the most essential industrial materials, utilized in the manufacture of pipes, accumulators, and as fuel and paint additives. Lead in plumbing can emit significant quantities of up to 2 mg/l into household water. Lead is known to accumulate in living creatures and cause poisoning symptoms in the human body[47]. Therefore, this dangerous pollutant that should be eliminated from water should be examined. The solution employed for lead adsorption has an average pH of 5, with the exception of

Tamarind wood AC in solution at pH 10. Tamarind wood AC with $ZnCl_2$ activation has the maximum surface area at 1322 m²/g, whereas tropical almond shells AC with CO_2 and steam activation has the highest adsorption capacity at 114.8 mg/g[44]. meanwhile, lead has been observed to be completely removed (100%) by watermelon peel AC, with oil palm shell AC following closely after at 99.8% removal efficiency[70].

Cadmium poses additional concern to very poisonous water. It is harmful to living species and aquatic ecosystems even at low concentrations, hence it is only allowed to be present in water at a concentration of 5-10 ppm[81]. Cadmium pollutants are mostly caused by battery manufacture or improper disposal of batteries, cadmium plating, and the use of cadmium- rich fertilizers. Waste effluents from these enterprises harm the water supply and the environment[80]. Oil palm shell AC was used to remove cadmium with a 99.5% efficiency[70]. Chemically activated date pits ACs effectively removed cadmium, with adsorption capacities ranging from 118.1 mg/g to 127.0 mg/g at pH 6 and temperatures of 25- 30 °C. Mercury has a low concentration in water, having a weight of 1 g/L. It may be found in aqueous waste from industry, just like lead and cadmium. NH₄NO₃ activated Pistachio wood wastes AC has a large surface area of 1448 m²/g and can adsorb mercury at a capacity of 201.095 mg/g at pH 6. vulgaris striata AC has a high adsorption capacity of 248.05 mg/g in a more acidic solution of pH 3. Physically activated Fe-supported walnut shell AC and Ceiba pentandra hulls AC have low chromium adsorption capacities (<30 mg/g), while chemically activated date pits and chestnut oak shells AC have higher adsorption capacities (120.5 mg/g and 85.47 mg/g, respectively). This demonstrates that chemical activation is preferred for chromium removal since it optimizes the adsorption process. Similarly, due to their poor adsorption capabilities, physically activated date pits AC have limited ability to extract iron, copper, and aluminum. Only chemically activated watermelon peel AC can remove iron and copper almost completely, with efficiencies of 91% and 99%[70]. The findings of experiment with GnZVI/PAC, PAC, and ACs from various predecessors. GnZVI/AC has a lesser surface area than PAC, but achieves a maximum adsorption of 53.48 mg/g, making it a superior adsorbent compared to PAC (18.18 mg/g) and other adsorbents that only remove < 50 mg/g of chromium from aqueous solution. They found that the explanation for this outcome was the loading of zero-valent iron particles, which produced the modification of functional groups and so increased the feasibility of the adsorbent and contaminants. As a result, nanoparticles play an important role in the removal of chromium from solution. A similar tendency was seen in another work, where Fe₃O₄/CSAC was utilized as an adsorbent and shown to be superior than CSAC alone for the removal of As(V) and As(III).

2. Removal of nonmetallic pollutants:

Although anions can be useful and important in human bodies, their excessive presence, such as fluoride, molybdate, and phosphate, can pose a hazard and be harmful to living things. Fluorosis has affected millions of individuals, particularly in underdeveloped nations, as a result of excessive fluoride levels in drinking water. discovered high fluoride levels in water (3.24 ppm) and linked it to fluorosis in youngsters. Similarly, molybdate in its anion form is easily absorbed by grazing cattle and accumulates in the food chain and water, which can be hazardous to grazers and carcinogenic to humans[82]. As a result, anion concentrations should be checked on a regular basis and tightly managed to ensure that they are within allowed limits in the water.

Three separate research investigations[82]-[83]that investigated the usage of farm waste coir pith with ZnCl2 activation for the elimination of anion contaminants in water such as thiocyanate, phosphate, and molybdate. Adsorption capabilities for thiocyanate and molybdate removal vary from 16-18 mg/g at pH 3.2 and 4-8, respectively. Phosphate removal has a lower capacity of 5.1 mg/g at pH 3-10. They found that, despite being a low-cost adsorbent, coir pith may be used as a precursor to make ACs for anion pollutant removal, and that chemisorption and ion exchange on AC surfaces affect adsorption capacities. Walnut shell AC, with its large surface area and adsorption capacity of 484.26 m²/g, effectively removes 52.67 mg/g of sulfur from aqueous solution. compared zirconium impregnated cashew nutshell AC to cashew nut shell AC that had been chemically activated with H2SO4.Zirconium impregnated Cashew nutshell AC (ZICNSC) has a higher removal effectiveness of 80.33% than just one cashew nutshell AC (72.67%), demonstrating the possibility of a modified AC for fluoride ion removal.

I.3.3.2. Organic contaminants from water

1. Color/Dye Removal

Dyes are widely used and applied in sectors such as paint, cosmetics, textiles, and paper goods. the textile sector is the leading cause of water contamination[84]. Out of the 3600 colors used in the industry, around 2-20% are lost in the effluent outflow for each manufacturing. As a result, dyes are one of the most concentrated and heavy contaminants in wastewater. These companies' effluents contain dyes, which can damage rivers and other water resources since they are poisonous and carcinogenic. They have the potential to destroy the marine ecosystem by reducing the photosynthesis of aquatic plants and animals. Furthermore, dye consumption might be harmful as it alters the human body.

There is a lot of promise in using activated carbon to extract colors from aqueous solutions. The polarity, solubility, molecular size, surface area, pore size, functional groups of AC, pH, and other ions in solution all affect the removal capacity. The pre-treatment procedure has the adsorption properties of organic compounds (dye) from the aqueous solution, which has a large number of mesopores and a high adsorption capacity, particularly for large molecules. ACs were obtained using the conservative steam-activation approach. It has been demonstrated that Acacia mangium and Acacia nilotica activated carbon can effectively remove a variety of dyes. The harmful textile dyes methyl orange (90.5%) and methylene blue (250 mg/g) may be eliminated by these AC.

Methylene Blue is the dye that is most frequently extracted from wastewater. According to reports, the majority of adsorption capabilities are greater than 100 mg/g. With a large surface area of 1430 m²/g, KOH activated distillers grains AC has the greatest adsorption of any AC utilized for methylene blue adsorption. It can adsorb 934.579 mg/g of methylene blue from aqueous solution. The adsorption process was carried out at pH 5.8 and 55 °C. N2H9PO4 was used to activate rice straw and Ramulus mori in order to provide AC for methylene blue adsorption. They had adsorption capacities of 314.1 mg/g and 129.5 mg/g, respectively, and surface areas of 1061 m²/g and 1154 m²/g.

Date pits have been used extensively to produce AC with chemical and physical activations for the removal of dyes such as maxilon blue, methyl orange, methylene blue, and remazol yellow. ZnCl₂-activated date pits AC performed best when used to adsorb methyl orange, with a maximum adsorption of 434.8 mg/g. KOH-activated date pits AC was next used to remove methylene blue, which adsorbed 316.1 mg/g of dye from aqueous solution. Lanaysn orange may be effectively removed from aqueous solutions using AC made from powdered bamboo cane, which has a very high adsorption capacity of 2600 mg/g[57]. Malachite green was adsorbed using ACs made from B. aethiopum flowers and chemically activated rambutan peels. Rambutan peel adsorbed 418.6 mg/g of dye from aqueous solution[44], but B. aethiopum flower AC adsorbed 48.23 mg/g of dye, which demonstrated a considerable difference in adsorption capabilities.

The use of green nanocomposites made from the synthesis of coconut husk and almond shell with Ag and WO₃ nanoparticles respectively, for the elimination of dye (methylene blue and rhodamine B) from aqueous solution was investigated by. Rhodamine B's adsorption capability with WO3/AC is considerable (1666.67 mg/g), but AgAC's removal of methylene blue is comparatively low (240 mg/g). Came to the conclusion that the high value was caused by WO₃ nanoparticle loading, which changed the adsorption processes for improved adsorption. This is comparable to okra waste AC, which only has a 321.5 mg/g adsorption capability[57]. Conversely, that the low value of AgAC

adsorption could be because nanoparticles only little affect AC's adsorption capacity. They came to the conclusion that the size, structure, and adsorption capacity of AC were unaffected by nanoparticles, it can be said that ACs generated by chemical and neutral activation are more effective in removing dye than those generated by physical activation. The significance of ACs' surface areas and functional groups for their interactions with the adsorbates was also determined by the results. Additionally, nanoparticles may not always be able to increase the adsorption capacity.

2. Elimination of phenolic compounds:

Phenolic compounds are mostly found in wastewater from the petrochemical and chemical industries. These contaminants are thought to pose a major danger to the aquatic ecosystem and living things since they are very poisonous and carcinogenic. Therefore, the content of phenolic compounds in water bodies has been rigorously restricted by environmental and health protection authorities and the removal of these contaminants is prioritized[47]. The World Health Organization (WHO) has set a maximum allowable concentration of 0.001 mg/L for phenols in drinking water[47], whereas the Environmental Protection Agency (EPA) has set a limit of 0.1 mg/L for similar pollutants in industrial effluents. Surface chemistry is more important than porosity for the adsorption of phenolic compounds by activated carbon because surface functionality increases significantly in comparison to the arrangement of pore sizes. Because of the π - π bond between the AC's surface and the adsorbent[44], the carboxyl and hydroxyl groups of the AC reserved the adsorption of phenol, which enhanced the AC's attraction to water. The donor-acceptor mechanism, in which the solute's aromatic rings act as the acceptor and the surface oxygen groups act as the electron donor[62], has been preserved by AC's removal of phenol and the phenolic compound. Phenol adsorption is influenced by the pH of the solution; at both high and low pH levels, the amount of adsorption reduces. The high pH of the phenols, which are mostly anionic, causes less adsorption because of the repulsion between the carbon surface and the anionic phenol.

Acidic solutions with lower pH levels produce protons, which combine with carbonyl groups to reduce adsorption. The many adsorbent types utilized to remove phenolic compounds, together with their adsorption capabilities and conditions. Investigated the use of argan nutshell AC for the adsorption of bisphenol A. According to reports, the maximal adsorption capability at 293 K is 1250 mg/g. When compared to commercial ACs, the nutshell AC demonstrated superior adsorption performance. Durian peel is another precursor utilized in this adsorption process. Even though the adsorption procedure persisted for a day, the adsorption efficiency with durian peel AC is extremely low (4.2 mg/g), with a clearance efficiency of 69%. Date pits, avocado kernels, kernaf rapeseed,

baobab wood, and Acacia seeds are examples of lignocellulosic biomass that has been utilized to produce AC for phenol adsorption. The H₃PO₄ activated baobab wood AC was shown to be the best adsorbent among these ACs. At an ideal pH of three and 50°C, maximum adsorption was achieved in 24 hours. That whereas non-acidic or basic functional groups improve adsorption, acidic surface functional groups on ACs may inhibit adsorption efficiency. Another study that chemically treated date pits AC with both H₃PO₄ and KOH for use in the elimination of phenolic chemicals supports this finding. While acidic-treated AC could only extract 142.9 mg/g of phenolic compounds from aqueous solution, basic-treated AC enhanced phenolic compound adsorption with 322.5 mg/g.

3. Elimination of pesticides:

Although pesticides are necessary in contemporary agriculture, excessive pesticide usage can degrade the quality of water. Common pesticides used in gardening and agriculture are 2,4- dichlorophenoxyacetic acid, bentazon, and carbofuran. Their maximum concentrations in water are established at certain amounts because they are mutagenic and carcinogenic, making them hazards to human health and the aquatic environment. For bentazon, carbofuran, and 2,4-dichlorophenoxyacetic acid, the acceptable levels in tap and drinkable water are 0.05 mg/L, 0.09 mg/L, and 0.1 mg/L[85]. These findings suggest that one of the best separating methods for removing pesticides from water supplies is adsorption. The percentage of organic matter, the continuous flow rate throughout the adsorption process, and the carbon dosages all affect how successfully the activated carbon adsorbs pesticides.

The widespread usage of date stones as precursors for pesticide adsorption. date stones AC's ability to adsorb several drin pesticides, including endrin, dieldrin, and aldrin, from aqueous solution. Maximum adsorption capacities were determined as 228.047, 295.305 and 373.228 mg/g for endrin, dieldrin, and aldrin, respectively, exhibiting a rise from endrin to aldrin. aldrin has the lowest solubility and so, it may be deduced that the rise of adsorption was related to the decrease in solubility of pesticides in water. investigated the physiochemically activated date seed ACs' adsorption capabilities. When date seeds were physiochemically treated with KOH and CO₂, the adsorption of bentazon and carbofuran under the same circumstances was 86.26 mg/g and 137.04 mg/g, respectively. They explained the difference in adsorption capabilities by pointing out that smaller carbofuran molecules had easier diffusion and adhesion to the AC surface than bentazon molecules. Similar findings were observed when the same experiment was conducted again in a different study: bentazon was found to have 78.13 mg/g and carbofuran to contain 175.4 mg/g. They also included an experiment on 2,4-dichloro-phenoxy acetic acid adsorption. This study shown that

AC could extract 175.4 mg/g of pesticides from aqueous solution[85]. Soy stalks, rapeseed stalks, maize cobs, and olive kernels were all physically activated to create ACs for the elimination of bromopropylate. All of the precursors utilized in this investigation had clearance efficiencies of 90–100%.

4. Elimination of pharmaceutical substances:

One of the new environmental contaminants is pharmaceutical chemicals, which are utilized extensively in aquaculture, agriculture, and human activities. The growing usage of medications throughout time has resulted in ongoing releases into the aquatic environment. They can be persistent in water and hence constitute a concern to the environment because of their high stability and hydrophilicity in water bodies. Pharmaceuticals can nonetheless have a negative impact on the environment even if their concentration in water is often very low, at a trace level. The bridging process, operating circumstances, adsorbent and precursor types, activation technique, and adsorbate (pharmaceutical) qualities all affect how well AC removes pharmaceutical substances. Also, the adsorption of activated carbon is significantly influenced by the operational approach, which includes the adsorbent dosage, adsorbate characteristics, operating temperature, solution pH, ionic capacity, and organic structure. The majority of researchers have demonstrated that the Langmuir and Freundlich isotherm models are driven by the adsorption of the medicinal ingredient by AC. The governing rate of the adsorption process in the carbon surface was being measured using kinetic modeling, collected the information from several studies that used various kinds of precursors to extract ibuprofen from aqueous solution. To make ACs, mugwort leaves, cork powder, mung bean husk, and olive stones were chemically and physically activated. The greatest result among these materials was recorded by steam activated cork powder, which was able to extract 378.1 mg/g of ibuprofen from water. This outcome may be compared to cork powder treated with K₂CO₃, and steam activated cork powder did in fact turn out to be better. With an adsorption capacity of 282.6 mg/g, CO₂ activated olive stones likewise performed better than the other ACs, whilst the other adsorbents only achieved adsorption capacities of less than 200 mg/g. The elimination of naproxen may also be examined between waste apricot AC and olive waste AC. After an adsorption period of 26 hours, H₃PO₄ treated olive waste AC was only able to remove 39.5 mg/g of the medication, but ZnCl₂ treated waste apricot AC removed 106.4 mg/g in 1 hour. Additionally, the adsorption of naproxen and ketoprofen was studied in olive waste. The adsorption capabilities of ACs were examined using the same precursor (olive wastes) and treatment (phosphoric acid). According to the findings, naproxen was more effectively adsorbed by olive waste AC (39.5 mg/g) than ketoprofen (24.7 mg/g). Given the unsatisfactory results, it is evident that olive waste AC was not an effective

adsorbent for medicinal chemicals. However, main paper mill sludge AC demonstrated good removal efficiencies of 75, 85, and 84% for SMX, CBZ, and PAR, respectively, and a high adsorption capacity of 405 mg/g towards paroxetine[57], making it an appropriate adsorbent. Clofibricacid (AC), tetracycline (TC), and paracetamol (PC) may be reduced by 83, 97.03, and 84%, respectively, using H3PO4 activated waste textiles (Cotton) AC. The removal of levofloxacin by date stones AC varied between 41.40 and 97.01 percent with 100.4 mg in one gram, while cyclamen persicum AC, which has a surface area of 799-880 m²/g, demonstrated favorable adsorption towards diclofenac. In a different study, Lagenaria vulgaris shell AC, which has a surface area of 665 m2/g, demonstrated very effective adsorption for ranitidine within the range of 93-99%.

I.3.3.3. Other pollutants from aqueous solution

That many contaminants, such as caffeine, aniline, suspended particles, etc., may be eliminated using activated carbon. Isocyanate is made using aniline, a crucial substance in the petrochemical sector. In the pharmaceutical, pesticide, and rubber industries, it is also utilized to produce accelerators and antioxidants. Teas, coffees, soft drinks, chocolate, and some types of sweets contain caffeine, an alkaloid that is utilized as a cardiac, cerebral, and respiratory stimulant. The average individual consumes around 200 mg of it daily, and if consumed, the body metabolizes it, excreting 1–10% of it in urine. ZnCl₂ outperforms H₃PO₄ in the removal of aniline from apricot stones AC; the values are 147 mg/g and 115 mg/g, respectively, with corresponding surface areas of 1111 and 1382 m²/g. Toluene could be removed by 874 mg/g from durian shell AC, p-nitrotoluene by 20 mg/g from orange peel AC, benzene by 212.77 mg/g from coconut shell AC, and formaldehyde by 245 mg/g from coffee leftovers AC[44]. However, steam activated bio-sorbent from oil palm mesocarp fiber AC removed suspended particles from palm oil mill effluent (POME) by 80%, while coconut shell AC activated by KOH eliminated 39% of suspended solids by the comparable surface area of 478 m2/g. Furthermore, KOH activated sugarcane bagasse AC and sea mango AC adsorbed NH₃-N at rates of 46.65 and 79.77%, respectively[57]. Aceh coffee grounds AC activated with hydrochloric acid reduced ammonia by 56%, whereas sugarcane bagasse AC reduced naphthalene by 119 mg/g with a surface area of 692 m²/g at pH 4. Pineapple leaves activated with phosphoric acid absorbed 155.5 mg of caffeine per gram, with a surface area of 1031 m²/g.

I.3.3.4. Gas adsorptions

In addition to liquid substances, activated carbon has been shown to be effective in gas adsorption since the combustion of fossil fuels emits greenhouse gases (GHG) and polluting gasses into the atmosphere as energy demand rises[86]-[87].AC is one of the most promising solid adsorbents for

adsorbing CO₂, CH₄, H₂S, NO₂, and H₂ gases due to its many advantages, including low cost, ease of regeneration, insensitivity to moisture, high gas adsorption capacity at normal atmospheric conditions, high surface area, adequate pore size distribution, high mechanical stability, and very low energy[88]. Pollutant gases were adsorbed on activated carbon via H-H interactions, dipole-dipole bonds, and even covalent connections between the gas and functional groups, resulting in an increase in efficiency[89]. The adsorption of hazardous gases by activated carbon is determined by the surface area, adsorption capacity, carbon micropore structure, and the solution's repeatability and processability[90].CO₂ adsorption is complicated due to adsorbent characteristics and surface groups. Activated carbon has a typical adsorption capability of roughly 5 wt.% at 298 K and 0.1 bar. The K+ ions in the functional groups performed an important role in CO₂ adsorption via electrostatic communication. The CO₂ adsorption performance has grown dramatically with increasing heating temperature up to 873 K. Micropores have the greatest impact on CO₂ adsorption at 1 bar, but pore size has a significant impact at lower pressures (less than 0.3 bar).

The application of activated carbon in NO₂ adsorption is prompted by the structure of the pores, as well as the kind and chemical organization of the AC surface. Hydrogen sulfide (H2S) is a colorless, poisonous, and odorous gas that poses a health risk to individuals and the environment at a concentration of 0.0047 ppm[91]. The most successful and well-known technology for H₂S removal is activated carbon, which uses modified carbon with caustic chemicals (KOH and NaOH) or oxidative chemicals (KI and KMnO₄) to elementalize the hydrogen sulfide gas. Because of their toxicity, the removal of SO₂ and NOx has recently received a lot of attention, and ACs appear to be more promising for eliminating these harmful gases due to their higher sorption capacity. It was discovered that impregnating metal oxides onto activated carbon effectively removes both SO2 and NOx. Sunflower seed AC outperforms almond shell AC in CO₂ adsorption (4.6 mmol/g vs. 2.7 mmol/g), equivalent to surface areas of 1790 and 862 m²/g, respectively. The activation agents for sunflower seed and almond shell AC were CO₂ and ZnCl₂, with similar surface areas of 870 m2/g. In addition, oil palm shell AC with a surface area of 1213 m² could remove CH₄ up to 13 cm³/g, while Agiricus fungus AC activated by KOH with a 2137 m²/g area could collect H2 by 4.7 wt% [44]. Phoenix dactylifera seeds activated by N2 removed up to 141.14 mg/g of CO₂, whereas coconut shell activated carbon removed up to 88.8% of H₂S.Walnut shell, AC, and plum stone AC had similar NO2 removal rates of 66.3 mg/g and 67 mg/g, respectively.CO₂, Na₂CO₃, and ZnCl₂ may activate oil palm shell AC, resulting in surface areas of 1213, 742.34, and 551.05 m²/g, respectively. These activated surfaces are highly efficient in removing methane and hydrogen sulfide.

Experimental part

Chapter II Materials and Methods

II.1. Introduction

This chapter includes the equipment, instruments, diverse procedures, items used, and experimental protocols.

II.2. Material used

- 1. Beakers (50mL, 100mL, 250mL, and 500mL).
- 2. Thermometer.
- 3. Erlenmeyer flask.
- 4. Magnetic bars.
- 5. Measuring cylinder.
- 6. Volumetric flask.
- 7. Spatula.
- 8. Test tubes (25 pieces).
- 9. Cuvette.

II.3. Equipment

1. Analytical balance

The weights were determined using an analytical balance.

2. Magnetic heating agitator

This device allows for quick and efficient mixing at a certain temperature that we can control.

3. Spectrophotometer

The UV-1900 is a high-performance double-beam UV-Vis spectrophotometer featuring Shimadzu's LO-RAY-LIGHTM diffraction grating technology. It has 1 nm resolution, low stray light and noise, and a scanning speed of 29,000 nm/min. The user-friendly multilingual interface enables a wide range of measurement modalities, including photometric, spectrum, quantitation, kinetics, time-course, and bio-methods. It provides high-accuracy quantitative analysis, detects low-concentration components, and meets Pharmacopeia requirements (JP, USP, EP).

It has network access for remote data checks (with additional memory) and can be used as a standalone unit with a color touch screen or with a PC running LabSolutions UV-Vis software. It now has a new CPU, which allows for faster response times, more efficient processing, and integrated data management.

3.1. Principles of Spectrometric Technique

The spectrometry approach is based on the ability of matter, and more specifically, certain molecules, to absorb specific radiation. It enables measurements to be taken using the Beer-Lambert law. This law for monochromatic radiation of wavelength λ provides a relation between the concentration C of a chemical entity in solution, its chemical nature, absorbance A, and the length of the path traveled 1 by the light in the solution.

$$A = \ln \frac{Io}{I} = \epsilon. l. C$$

With:

- A: absorbance.
- **E**: molar absorptivity or absorption coefficient
- L: length of the Cuvette.
- C: concentration
- Io: the intensity of the incident monochromatic light beam and I the intensity of the emerging light beam

II.4. Characterization methods

Infrared spectroscopy

Infrared (IR) spectroscopy is a typical technique for identifying organisms on solid surfaces. The material absorbs or reflects electromagnetic radiation in the infrared region (2.5-25 μ m). A material with a certain chemical composition and structure will exhibit a collection of distinct absorption bands that indicate the nature, quantity, and orientation of chemical bonds.

II.5. Used chemical products

• Phosphoric acid (H₃PO₄).

II.5.1 adsorbats used (pollutants)

This study focuses on the adsorption of two particular dyes, Methylene Blue and Methyl Orange. These colors are widely used in a variety of industries, including cosmetics, textiles, medicines, food, and papermaking. They were chosen as exemplary examples of medium-sized organic contaminants.

a. Methylene Blue (BM)

Methylene Blue dye (CI 52015) is a cationic dye with the chemical formula $C_{16}H_{18}N_3SCl$. It belongs to the Xanthine family. It is widely utilized in a variety of applications, including silk, cotton, and wood dyeing, and also for temporary paper coloring. Methylene blue is also utilized for chemical, biological, and medicinal purposes. It's a dark blue crystalline powder. The characteristics are given in the table below.

Urelene blue, Provayblue, Proveblue. Trade names **IUPAC** Name [7-(dimethylamino)phenothiazin-3-ylidene]-dimethylazanium;chloride Molecular Formula $C_{16}H_{18}N_3SCl$ Molecular structure Molecular Weight 319.9 g/mol 668 nm λmax family Phenothiazine pН 6 190°C Melting point

Table II-1: Characteristics of Methylene Blue

b. Methyl Orange (MO)

The colorant methyl orange is an anionic organic compound with the general formula $C_{14}H_{14}N_3NaO_3S$, and it's a popular pH indicator in titration because to its apparent and noticeable color variation at different pH levels. In an acidic condition, methyl orange turns red, while in a basic medium it turns yellow, its belongs to the azoic family.

Table II-2: Characteristics of methyl orange.

Trade names	helianthine, Poivrier orange, gold orange or orange III			
IUPAC Name	sodium;4-[[4-(dimethylamino)phenyl]diazenyl]benzenesulfonate			
Molecular Formula	$C_{14}H_{14}N_3NaO_3S$			
Molecular structure	N-N-N-N-N-N-N-N-N-N-N-N-N-N-N-N-N-N-N-			
Molecular Weight	327.34 g/mol			
λmax	505 nm			
family	Azo dye			
рН	3.1-4.4			
Melting point	>300 °C			

II.6 Calibration Curve.

to create a calibration curve that shows the dyes' optical densities (BM and MO) in relation to their concentrations. First, we'll get the mother solution ready. This will enable us to use the following relationship to prepare the daughter solutions using the dilution method:

$$C_1 V_1 = C_2 V$$

With:

- C1: Concentration of the mother solution.

- V1: Volume of the mother solution.

- C2: Concentration of the daughter solution.

- V: Volume of the daughter solution.

II.7. Experimental Protocol

II.7.1. Adsorbents

In our experimental work, we used activated (AC) as an adsorbent.

II.7.1.1. Activated carbon preparation (AC)

After being chopped down, Washingtonia stems were regularly cleaned to get rid of contaminants, and then they were treated with warm water to get rid of any remaining oil. After being ground and sieved to a powder with particles smaller than 50 micrometers, they were dried for 24 hours at 110°C. After that, the product was activated with phosphoric acid (H₃PO₄) and heated to 700 °C for an hour at a rate of 5 °C per minute.

Finally, the latter was washed several times with distilled water to obtain a neutral pH, the product was dried again at 110°C for 48 hours to obtain activated carbon.

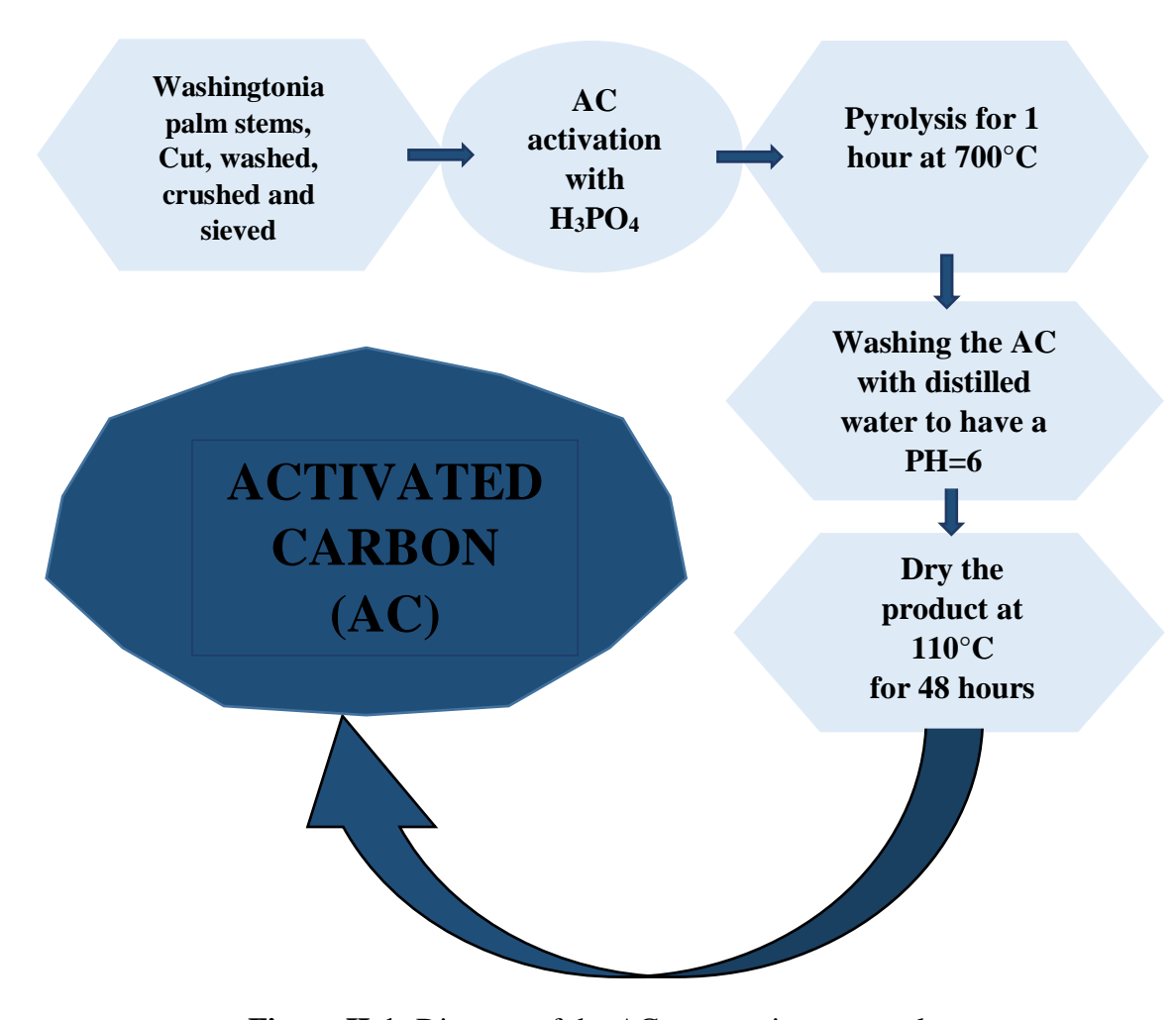


Figure II-1: Diagram of the AC preparation protocol.

II.7.2. Preparation of stock (mother) solutions of the dyes MO and BM

The mother solutions of the two colorants, MO and BM, were generated with a concentration of 30mg/l following the next steps.

- Weighed 30 mg MO and BM.
- Each quantity was poured into a 1 L graduated flask with a funnel to avoid mass loss.

Chapter II: Materials and Methods

- A little distilled water was placed into each flask and swirled with a magnetic bar until the solution was entirely dissolved.
- Next, the flasks were filled with distilled water to the fill line.

II.7.2.2. Preparation of daughter solutions

- -The stock solution was properly diluted to concentrations (0.9; 1.87; 3.75; 7.5; 15; 30 mg/l).
- -The volumes corresponding to these concentrations were poured into a 25 ml graduated flask.
- -The volume was topped up with distilled water to the to the fill line 1.

We have at our disposal five daughter solutions S1, S2, S3, S4, and S5; and the stock solution (S0). These solutions, with concentrations of 0.9; 1.87; 3.75; 7.5; 15; 30 mg/l, allowed us to obtain the Abs=f (conc) calibration curve for each dye or pollutant (Figure II-1 and Figure II-2) by spectroscopic analysis using a computer-controlled SHIMADZU UV-1900 UV-visible device. These calibration curves then make it possible to know the unknown concentration, the absorbance of the dyes or pollutants and the correlation coefficient R2.

Table II-3: Absorbance value

	Méthyle Orange								
C0 (mg/L)	0	30	15	7.5	3.5	1.87	0.9		
(mg/L) Abs	0	2,135	1,055	0,531	0,263	0,131	0,07		
	Methylene Blue								
C0 (mg/L)	0	30	15	7.5	3.5	1.87	0.9		
Abs	0	2,318	1,118	0,57	0,227	0,131	2,318		

Chapter II: Materials and Methods

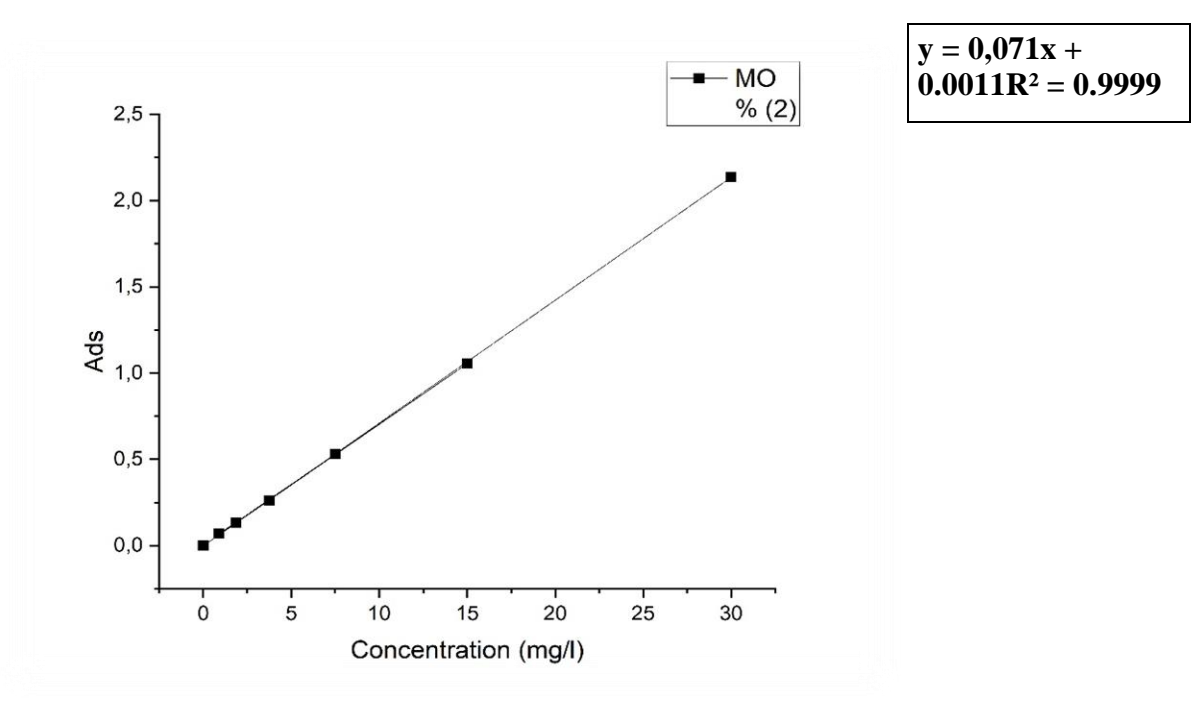
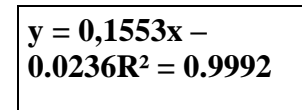


Figure II-2: Calibration curve of Methyl Orange

The equation of the straight line giving the absorbance A as a function of the concentration of methyl orange is: A=0.071C, with a regression coefficient R²=1 which can be considered a very good linear fit. This equation is used to calculate the concentration of an unknown solution of methyl orange.

Chapter II: Materials and Methods



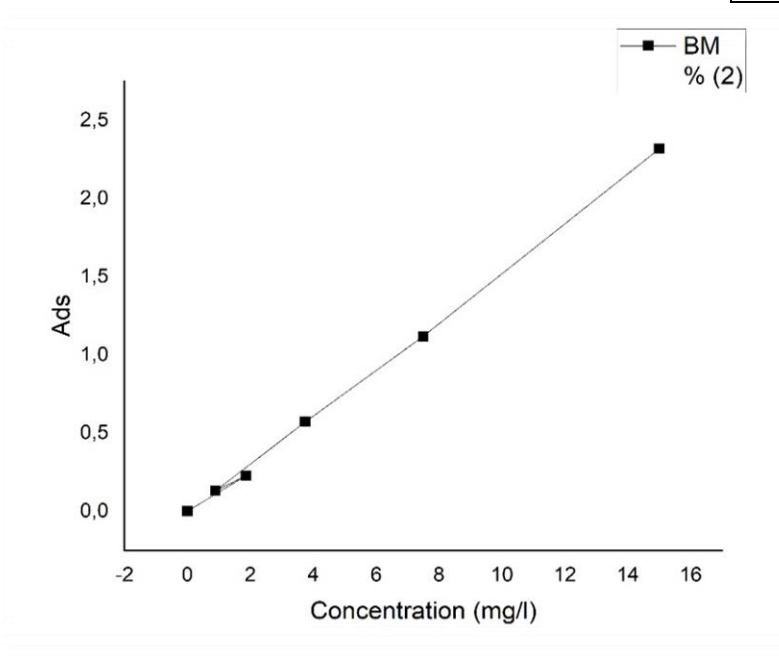


Figure II-3: Calibration curve of Methylene Blue

For methylene blue, the absorbance A plot as a function of concentration is A=0.1553C, with a regression coefficient R²=0.9992, which can be considered a very good linear fit. This equation is used to calculate the concentration of an unknown solution of methylene blue.

Chapter III

Results and Discussion

III.1. Introduction

In this chapter, we describe the properties of our activated carbon sample and the results of Methylene Blue and Methyl Orange adsorption in an aqueous media. We begin by investigating several factors such as contact duration, starting adsorbate concentration, and temperature, followed by the application of various models to describe the experimental results of adsorption kinetics and isotherms, and finally, a thermodynamic study of the adsorption equilibrium.

III.2. Characterization of Activated Carbon

III.2.1. FTIR analysis

The IRTF spectra of our generated activated carbon sample offer us with information on the vibrational state of the functional groups on the surface of the material investigated, providing the following information:

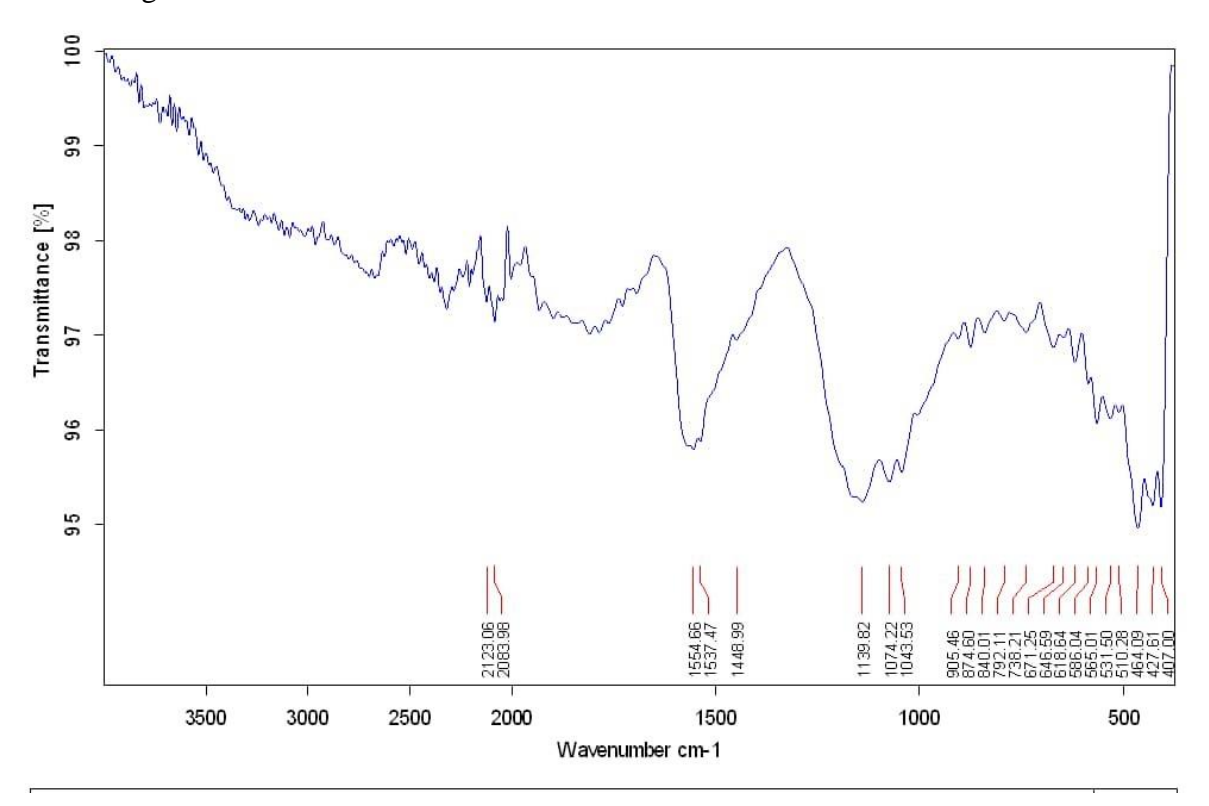


Figure III.1: FTIR spectra of activated carbon

• The band between 2083.98 and 2123.06 represents stretching vibrations of C≡C groups.

Chapter III: Results and Discussion

- The presence of an aromatic ring is indicated by a band at 1554.56 cm-1, which corresponds to the stretching of the C=C bond.
- At 1043.53 cm⁻¹, we see a peak due to the stretching movement of C-O, which is typical of epoxide structures or aromatic ethers.
- The bands at 407 to 905.46 are caused by deformation vibrations of C-H in benzene derivatives.

III.3. Kinetics of the adsorption of BM and MO dyes on activated carbon

The kinetic study was carried out to determine the contact time at which the elimination of our two pollutants (Methylene Blue and Methyl Orange) reached their maximums (the time required to reach adsorption equilibrium).

III.3.1. Kinetic study protocol

For this, we used a volume of 200ml of the mother solution (30mg/l) for the two dyes and added 100mg of activated carbon weighed on a scale. Poured into a beaker, the mixture is magnetically stirred at room temperature for 120 minutes, with a sample taken every 5 minutes. The collected solution is placed into a test tube that has been well-numbered according to the sample time (t).

- ❖ The solid phase and the liquid phase are separated by centrifugation.
- **!** Methylene blue is analyzed at a wavelength $\lambda = 665$ nm, and for methyl orange, the wavelength $\lambda = 547$ nm.

The amount absorbed is calculated by the following equation:

$$Q = \frac{(C_0 - Ce)v}{w}$$

With:

- **Q:** Quantity adsorbed per gram of adsorbent (mg/g).
- C₀: Initial concentration (mg/L).
- C_e: Equilibrium concentration (mg/L).
- **V:** Volume of the solution (L).
- w: weight of the adsorbate (g).

The percentage of the amount of dye adsorbed is calculated as follows:

$$\mathbf{R} (\%) = \frac{(C_0 - Ce) * 100}{C_0}$$

The results obtained were utilized to calculate the equilibrium time and then to derive the adsorption kinetics model (pseudo-first and pseudo-second order).

III.3.2 Effect of contact time

The analysis of the evolution of the absorbed quantity as a function of time Q=f(t) enables the determination of the equilibrium time. This time corresponding to saturation.

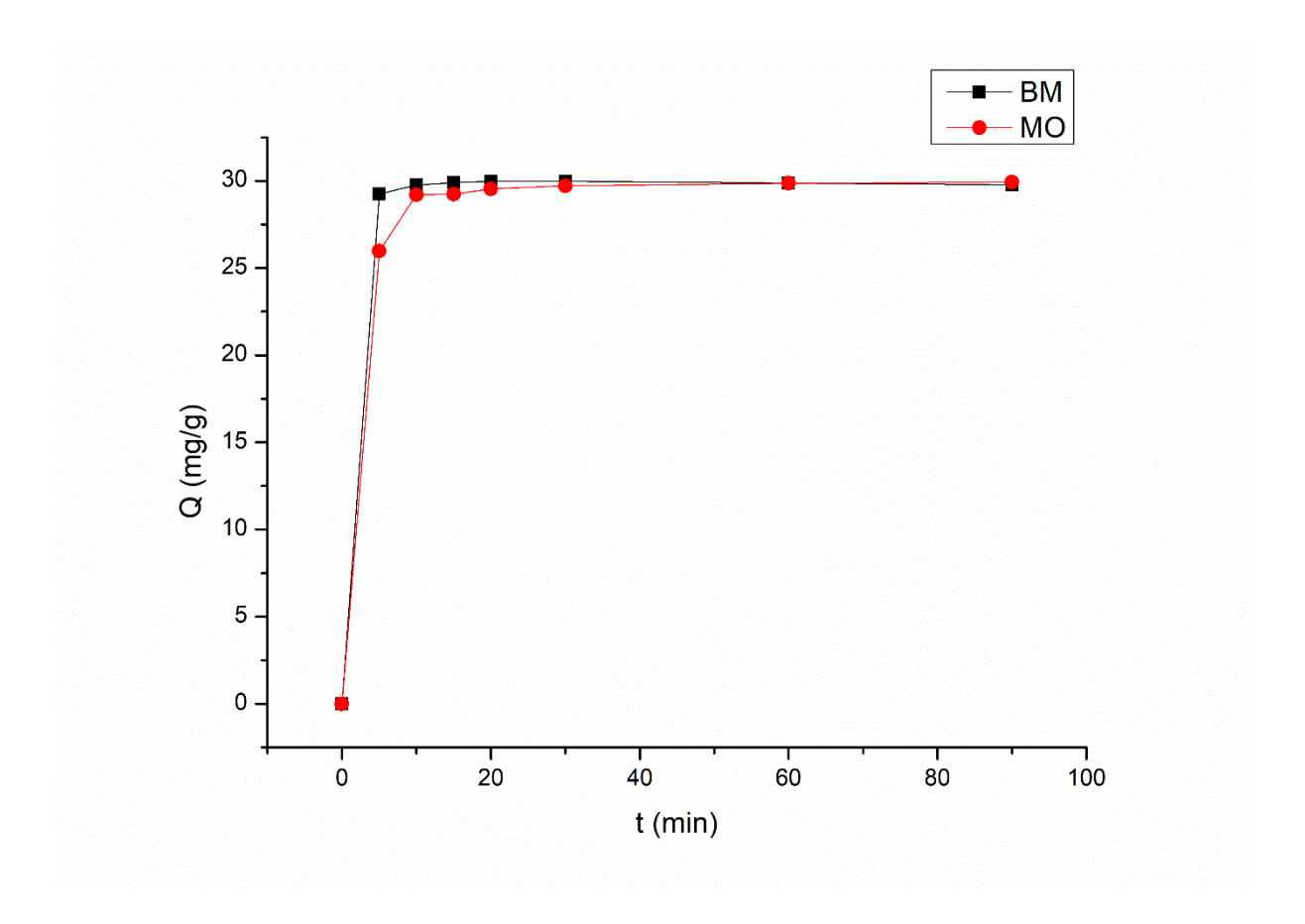


Figure III.2: Kinetic adsorption curve of BM and MO.

The curves are classified into two parts:

First part: approximately 5 minutes of contact time, we have (98.75% for BM and 93.28% for MO).

Second part: at half an hour for BM and MO, we have (99.98% of BM) and (99.53% of MO).

Chapter III: Results and Discussion

The results (Figure III.2) reveal that the adsorption kinetics is quite fast in the initial few minutes (first part), which explains the large availability of active sites on the surface of the activated carbon (the adsorbent) and indicating a high affinity between the adsorbent and the dyes. The adsorption kinetics become extremely sluggish (second part) with both curves plateauing around the 30-minute mark, due to the saturation of active sites on the surface of the activated carbon. Adsorption equilibrium is achieved after approximately 30 minutes for both MO and BM, BM reaches a slightly higher equilibrium adsorption capacity (~29.98 mg/g), whereas MO stabilizes at approximately 29.72 mg/g.

III.4. Modeling the adsorption kinetics of BM and MO dyes on activated carbon

In this part, we used the first and second order kinetic laws, in order to verify the models of the kinetic curves applicable to our experimental work.

I. Pseudo-first-order (PFO) model:

It is expressed by the following equation:

$$\frac{\mathrm{dqt}}{\mathrm{dt}} = k_1 \, (\mathrm{qe} - \mathrm{qt})$$

With:

- ❖ k₁: Rate constant for pseudo-first-order kinetics (min⁻¹).
- q_e: Adsorption quantity at equilibrium (mg/g).
- ❖ q_t: Adsorption quantity at time t (mg/g).

Integrating the previous equation for the boundary conditions: q = 0 at t = 0 gives:

$$qt = qe(1 - e^{-k1t})$$

II. Pseudo-second-order (PSO) model:

It is represented by:

$$\frac{dQt}{dt} = K_2(qe - qt)^2$$

$$ln(qe-qt) = lnqeK_2t$$

 K_2 : The rate constant for pseudo-second-order kinetics (mg·g⁻¹·min⁻¹).

The integration of the previous equation for the boundary conditions: q = 0 at t = 0 gives:

$$\frac{1}{\mathbf{q}\mathbf{e} - \mathbf{q}t} = \frac{1}{qe} + k_2 t$$

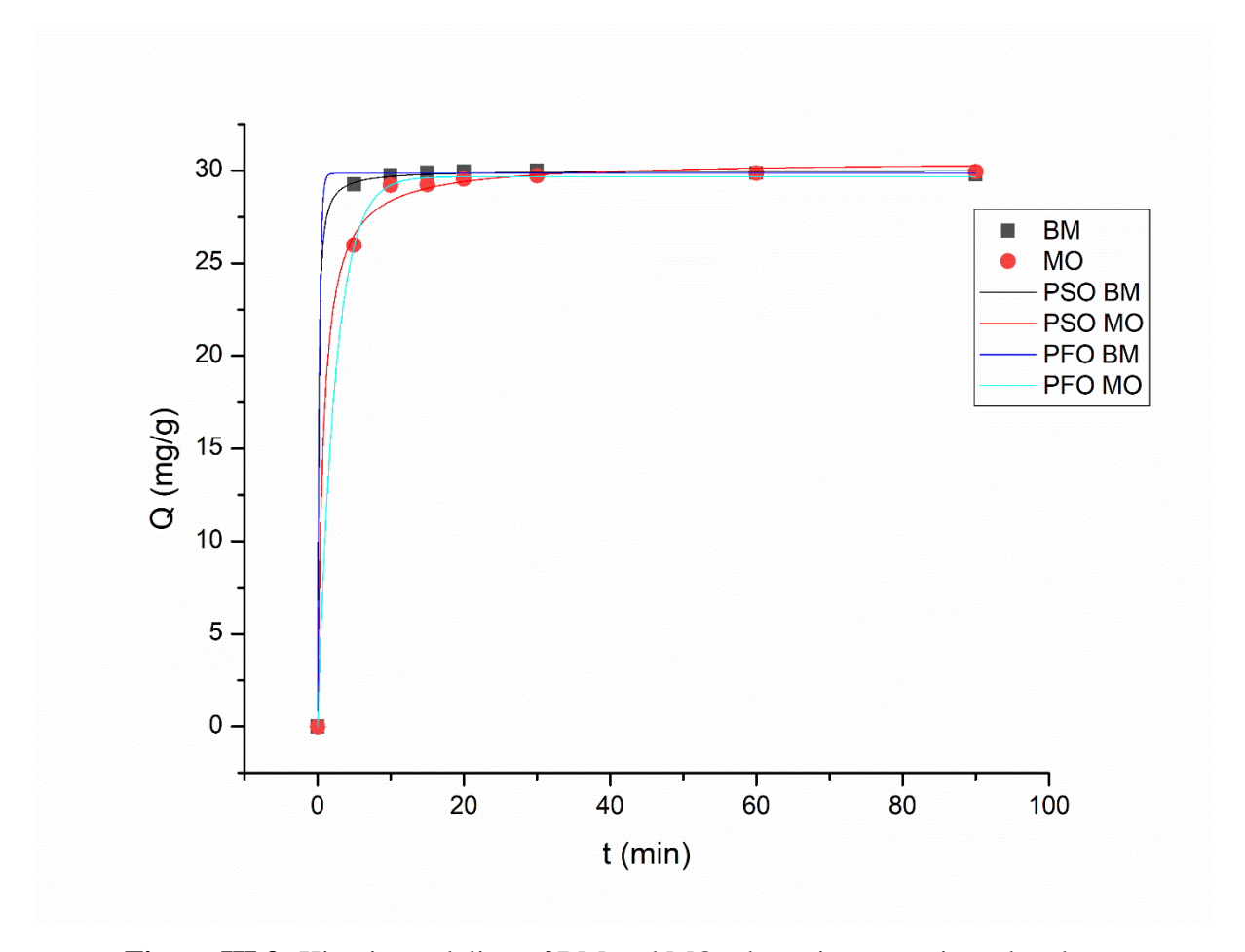


Figure III.3: Kinetic modeling of BM and MO adsorption on activated carbon.

Table III.1: Parameter values of the two kinetic models.

	Model								
Dyes		First or	rder	Second order					
	Qmax	\mathbf{K}_1	R ²	Qmax	K ₂	R ²			
BM	29.844	4.018	0.91581	30,02	0,293	0,99988			
МО	29.678	0.415	0,99965	30.51	0,043	0,99836			

Chapter III: Results and Discussion

We have:

Qmax: Maximum adsorption capacity.

❖ **K**₁: First-order rate constant.

❖ K₂: Second-order rate constant.

❖ R²: Correlation coefficient, which indicates the goodness of fit for each model.

According to these results of table, we observe that the correlation coefficients relative to the second order model for BM are very close to 1 than correlation coefficients relative to the first order for BM, and also we observe that the correlation coefficients relative to the first order model for MO are very close to 1 than the correlation coefficients relative to the second order model for MO, this confirms the validity of this two models. The second order model is favorable for the adsorption of BM, and the first model is favorable for the adsorption of MO.

III.5 Adsorption isotherm

Adsorption isotherms are critical to understanding the adsorption mechanism. In general, they provide information about adsorbent enhancement as well as the adsorption mode, which might be monolayer or multilayer.

III.5.1 Protocol of the isothermal study

1) We made solutions with varying concentrations (600mg/l, 400mg/l, 200mg/l, 100mg/l, 50mg/l, 25mg/l, 10mg/l, and 5mg/l) and poured 50ml of each into eight 50ml beakers labeled with the concentration.

2) 50mg of activated carbon was added to each beaker.

3) The solutions are heated to various temperatures (20°C, 35°C, and 50°C) and stirred for 250 minutes using a magnetic stirrer.

The procedure was repeated at each temperature.

Then, the samples of the solutions were filtered and analyzed using UV-Visible adsorption spectroscopy.

The results obtained from this study were used to plot adsorption isotherm curves, assess the effect of initial concentration, verify the validity of the Langmuir and Freundlich models, and study thermodynamics.

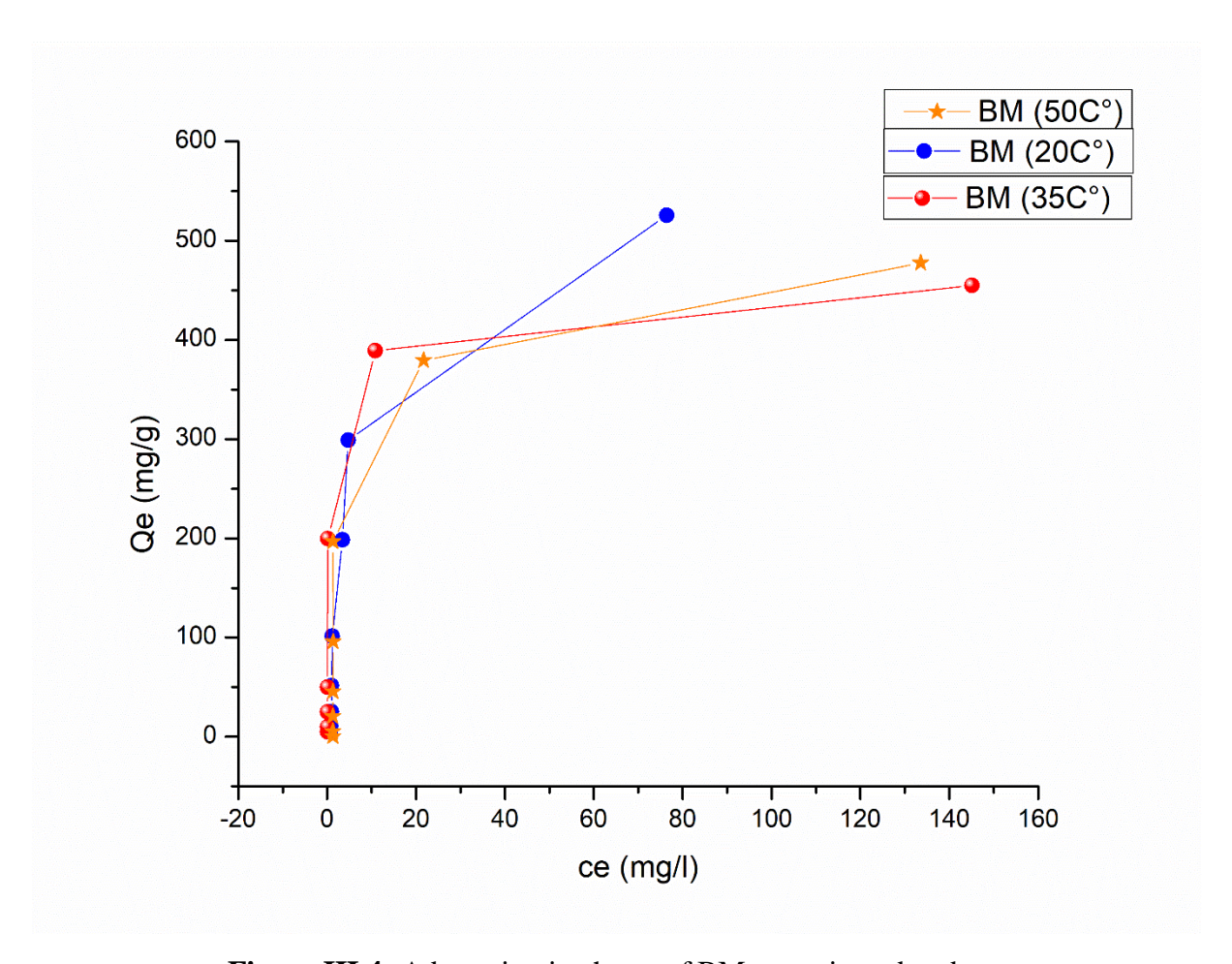


Figure III.4: Adsorption isotherm of BM on activated carbon.

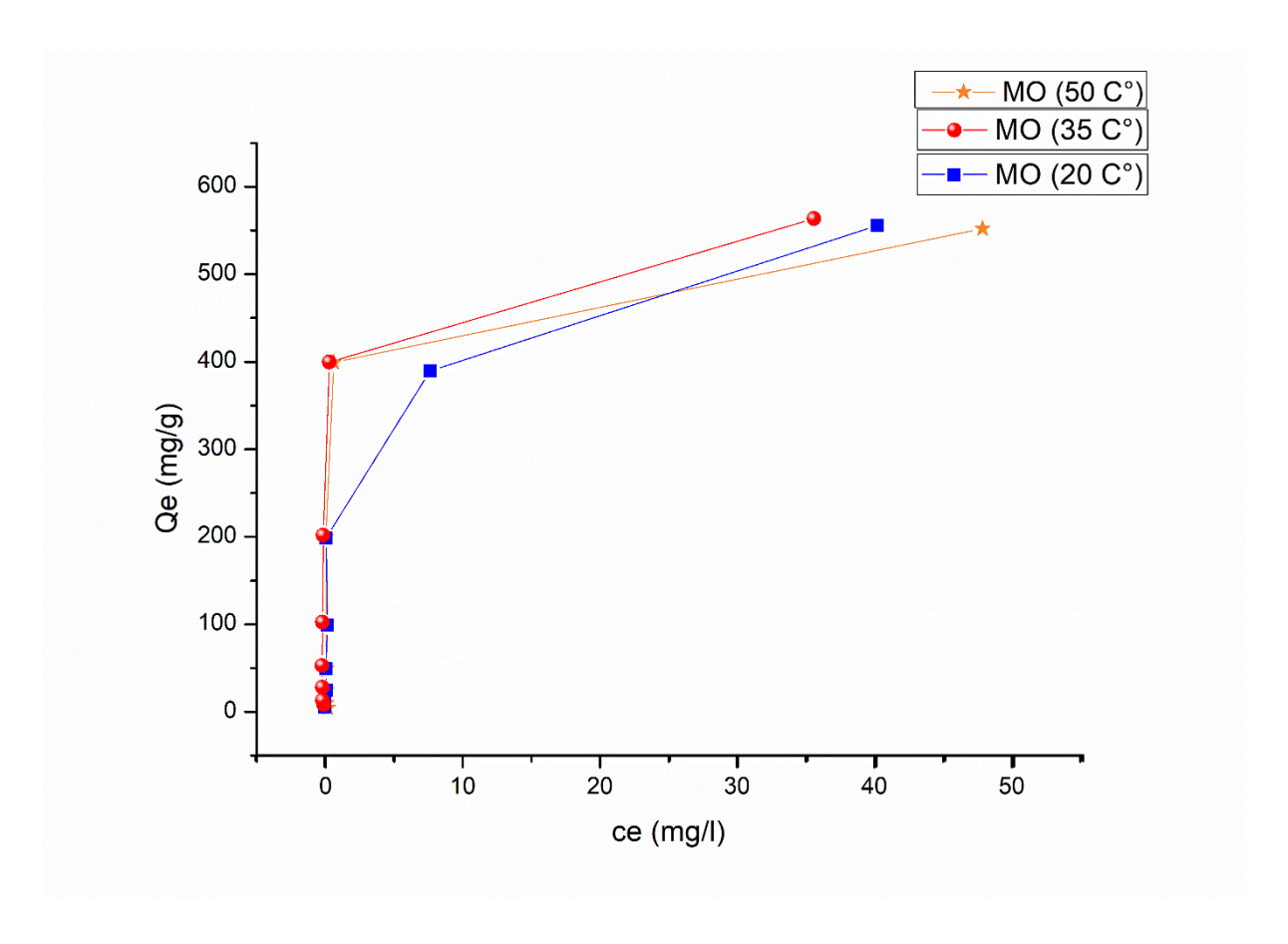


Figure III.5: Adsorption isotherm of MO on activated carbon.

According to Giles' classification, the obtained curves indicate that the dyes' adsorption isotherms on our activated carbon are type L and H with BM and MO.

III.5.2 Effect of Initial Concentration

The investigation of the impact of starting concentrations of MB and MO on the adsorption capacity of activated carbon at Constant temperature was conducted with initial concentrations ranging from 5 to 600 mg/l at the temperature of 50°C

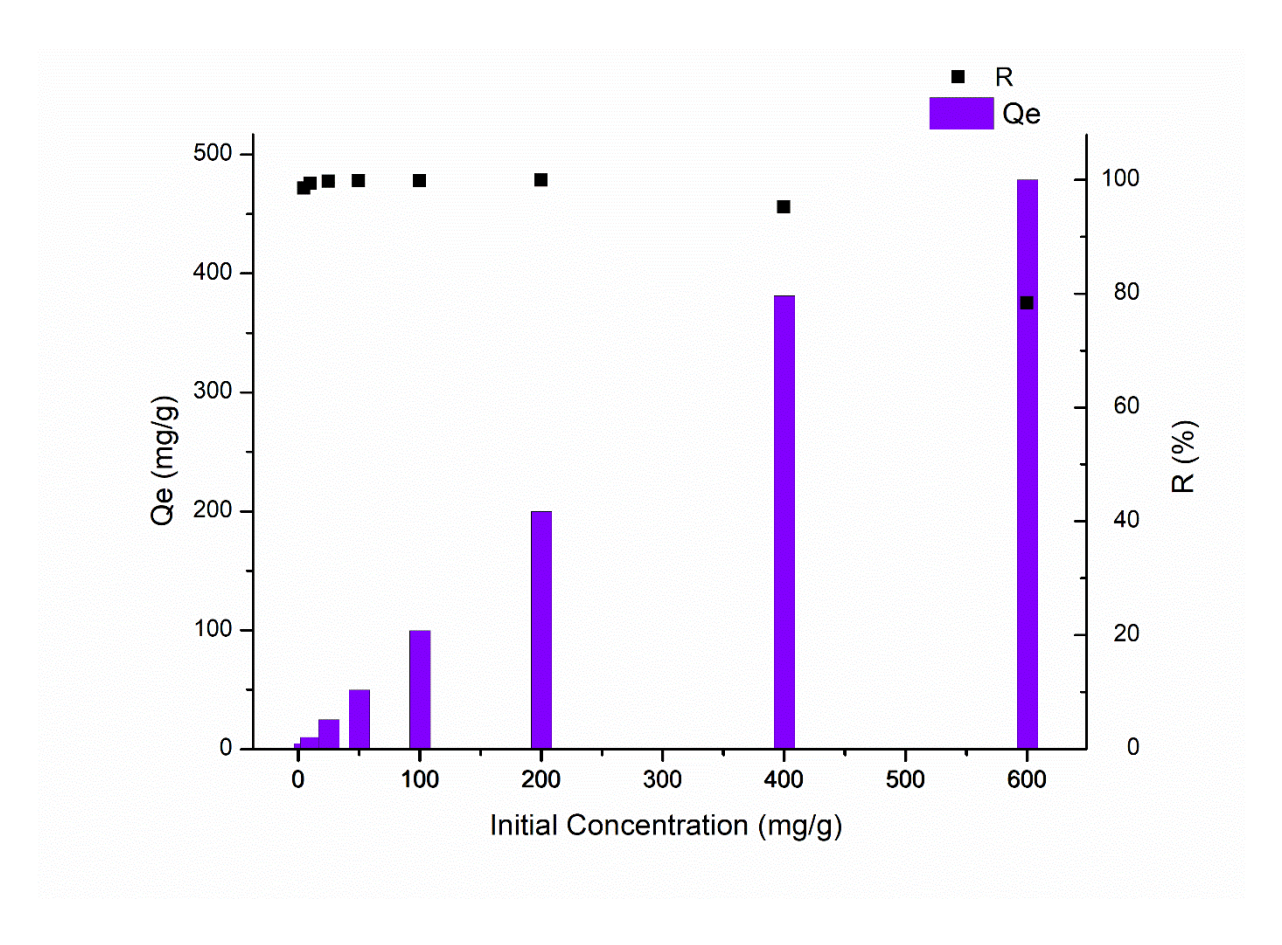


Figure III.6: the impact of initial dye (BM) concentration on adsorption capacity and removal percentage at 50°C

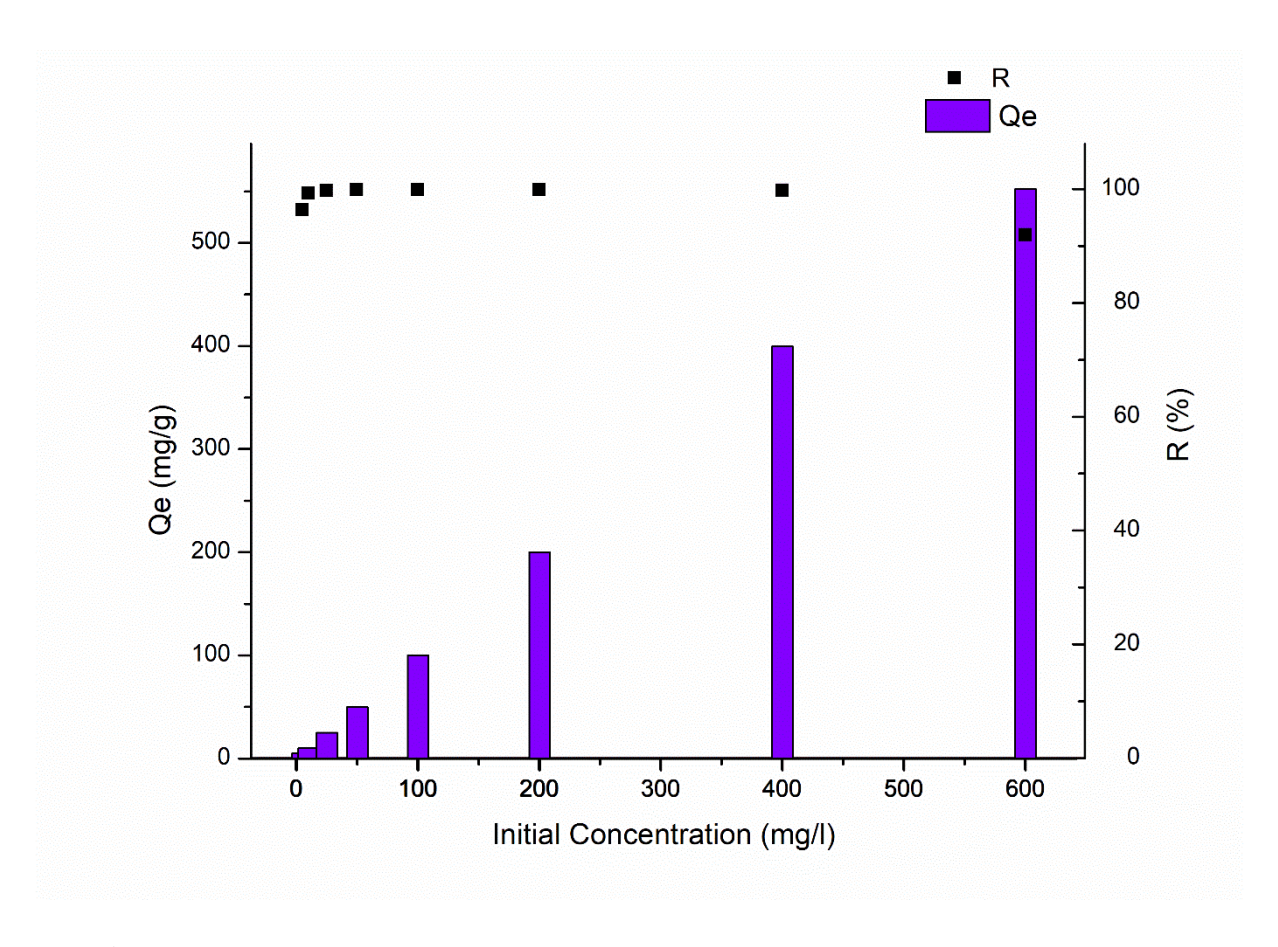


Figure III.7: the impact of initial dye (MO) concentration on adsorption capacity and removal percentage at 50°C

We observed that the adsorption capacity increased with the initial dye concentration. This is explained by the fact that, at lower concentrations, all the BM or MO molecules present in the adsorption medium can interact with the binding sites on the adsorbent surface. Thus, higher adsorption amounts were obtained at higher initial concentrations. This increase is attributed to the ratio between the available active sites and the initial number of adsorbate molecules, and we observe at higher initial concentration, the removal percentage decreases a little bit due to the saturation of active sites.

III.5.3 Effect of temperature

Temperature is an important component to consider in adsorption research since the process involves heat transfer between a liquid and solid phase, which can be exothermic or endothermic.

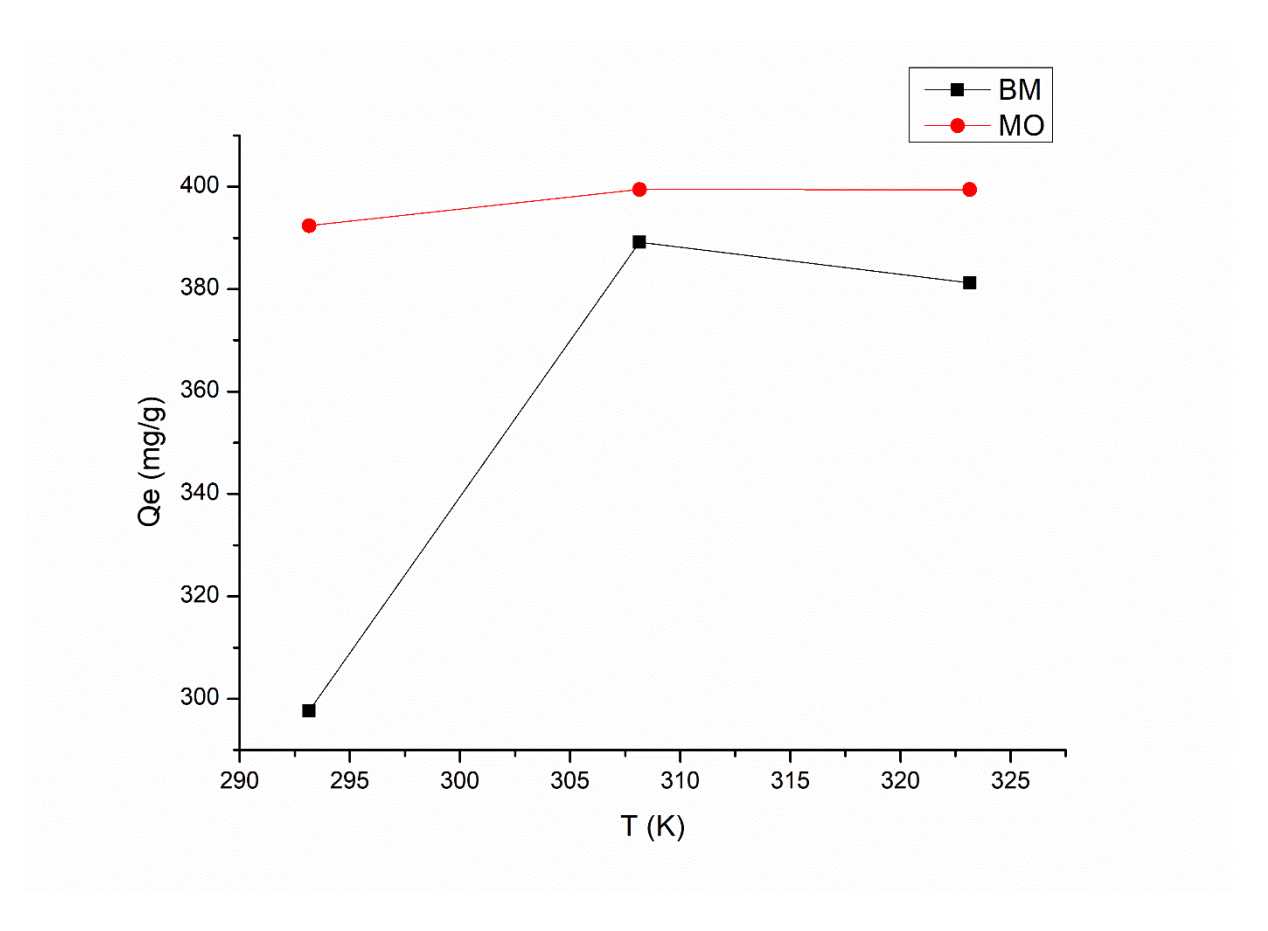


Figure III.8: Effect of temperature on the adsorption of BM and MO (C0=400m/g; t=120min).

For BM, the adsorption capacity goes up sharply from 297.65 mg/g at 293.15 K to 389.15 mg/g at 308.15 K, then drops slightly to 381.20 mg/g at 323.15 K. The sharp rise in Qe suggests that creased temperature enhances MB diffusion and surface interaction, indicating an endothermic adsorption process. And for MO Between 293.15 K and 308.15 K, there was a continuous, small rise in adsorption from 392.37 mg/g to 399.47 mg/g. At 323.15 K, there was almost no change. That also indicating an endothermic adsorption process, the constant findings at higher temperatures suggest that there isn't much temperature dependence. This could be because of strong interactions between the adsorbate and adsorbent or because the surface reached equilibrium early.

III.6 Modeling of the adsorption isotherm

1. Langmuir Model

The isotherm is represented by the following equation:

$$Qe = \frac{\text{Qm.KL.Ce}}{1 + \text{KL.Ce}}$$

2. Freundlich Model:

The isotherm is represented by the following equation:

$$Qe = KfCe^{1.n-1}$$
.

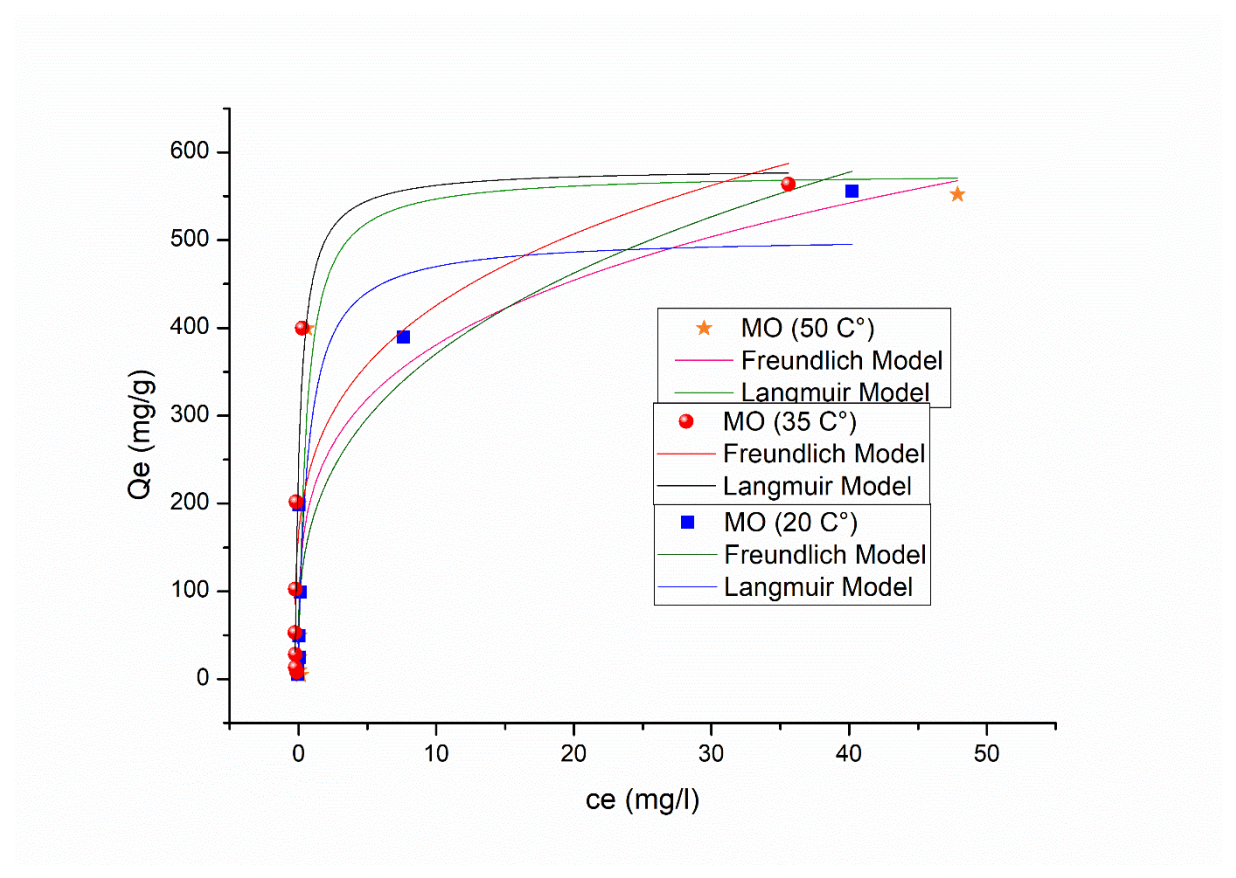


Figure III.9: Isothermal modeling of the adsorption of MO on activated carbon.

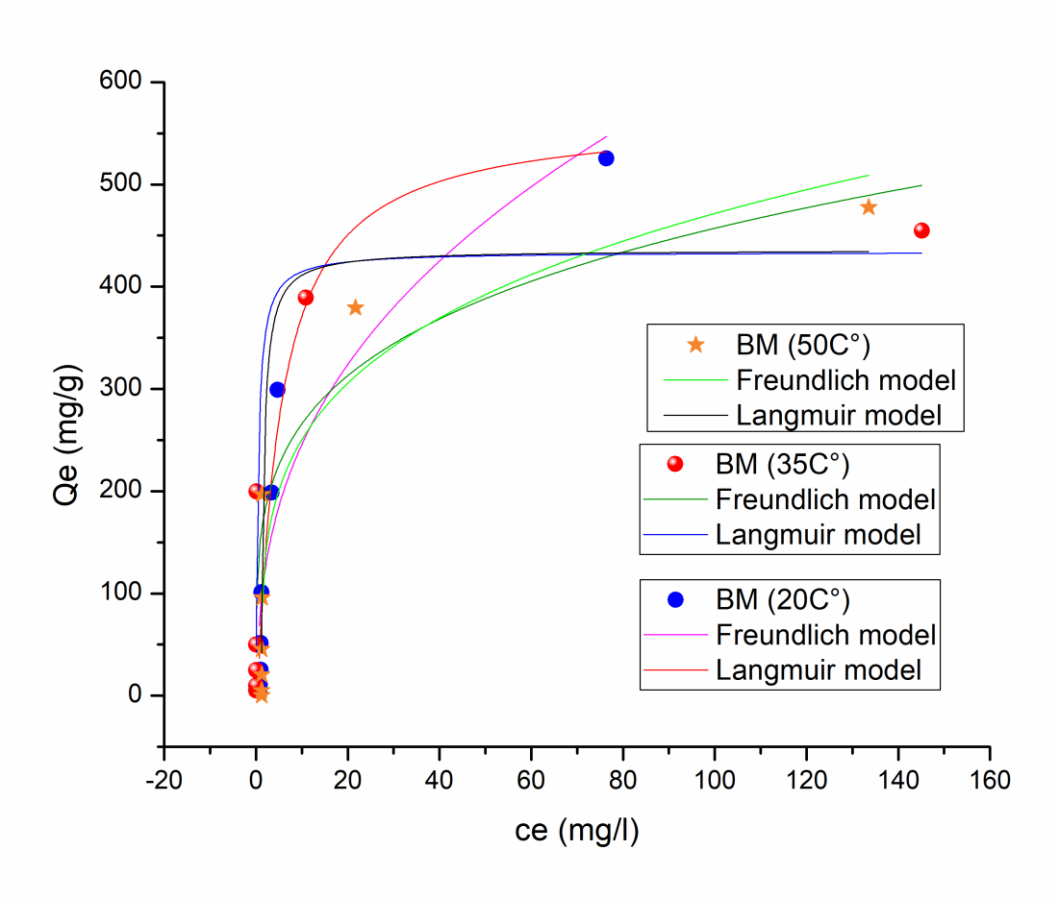


Figure III.10: Isothermal modeling of the adsorption of BM on activated carbon.

Table III.2: Adsorption modeling by the Langmuir and Freundlich models of BM.

	BM isotherms								
	Langmuir			Freundlich					
Temperature	Q _{max} (mg/g)	K _L	R ²	K _F	1/nf	R ²			
T (°C)									
20	565.98	0,195	0.97	101.68	0.38	0.87			
35	434.14	2.13	0.92	154.53	0.23	0.80			
50	437.30	2.05	0,87	147.39	0.25	0.85			

Chapter III: Results and Discussion

Table III.3: Adsorption modeling by the Langmuir and Freundlich models of MO

		MO isotherms							
		Langmuir		Freundlich					
Temperature	Q _{max} (mg/g)	K_L	\mathbb{R}^2	K_{F}	1/nf	\mathbb{R}^2			
T (°C)									
20	507	1.37	0.9	178.08	032	0.91			
35	583.41	2.75	0.88	233.12	0.25	0.74			
50	570.67	1.81	0.75	211.66	0.25	0.67			

The results from both models indicate that the Langmuir isotherm more accurately characterizes the adsorption of Methylene Blue and Methyl Orange on activated carbon. This suggests that the adsorption of dyes on the surface of activated carbon is a monolayer adsorption.

III.7 Thermodynamic Study

This section is based on a concentration of 400 mg/l among the solutions studied in the adsorption isotherm.

The thermodynamic parameters, Gibbs free energy (ΔG^0), enthalpy change (ΔH^0), and entropy change (ΔS^0), were calculated to assess the nature of the adsorption process.

 \bullet ΔG^0 can be determined from the following equation:

$$\Delta G^0 = -RTln(K_d)$$

With:

• **K**_d: Thermodynamic equilibrium constant.

• T(K): Temperature.

• **R**: Universal gas constant $(8.32 \text{ J mol}^{-1}\text{K}^{-1})$.

• The relationship between ΔG^0 , ΔH^0 and ΔS^0 is expressed by the following equations:

$$\Delta G^0 = \Delta H^0$$
-T ΔS^0

$$Ln(Kd) = -\frac{\Delta H^0}{RT} + \frac{\Delta S^0}{R}$$

With:

• ΔH^0 : Enthalpy change (kJ mol⁻¹).

• ΔS^0 : Entropy change (J mol⁻¹ K⁻¹).

• ΔG^0 : Gibbs free energy (kJ mol⁻¹).

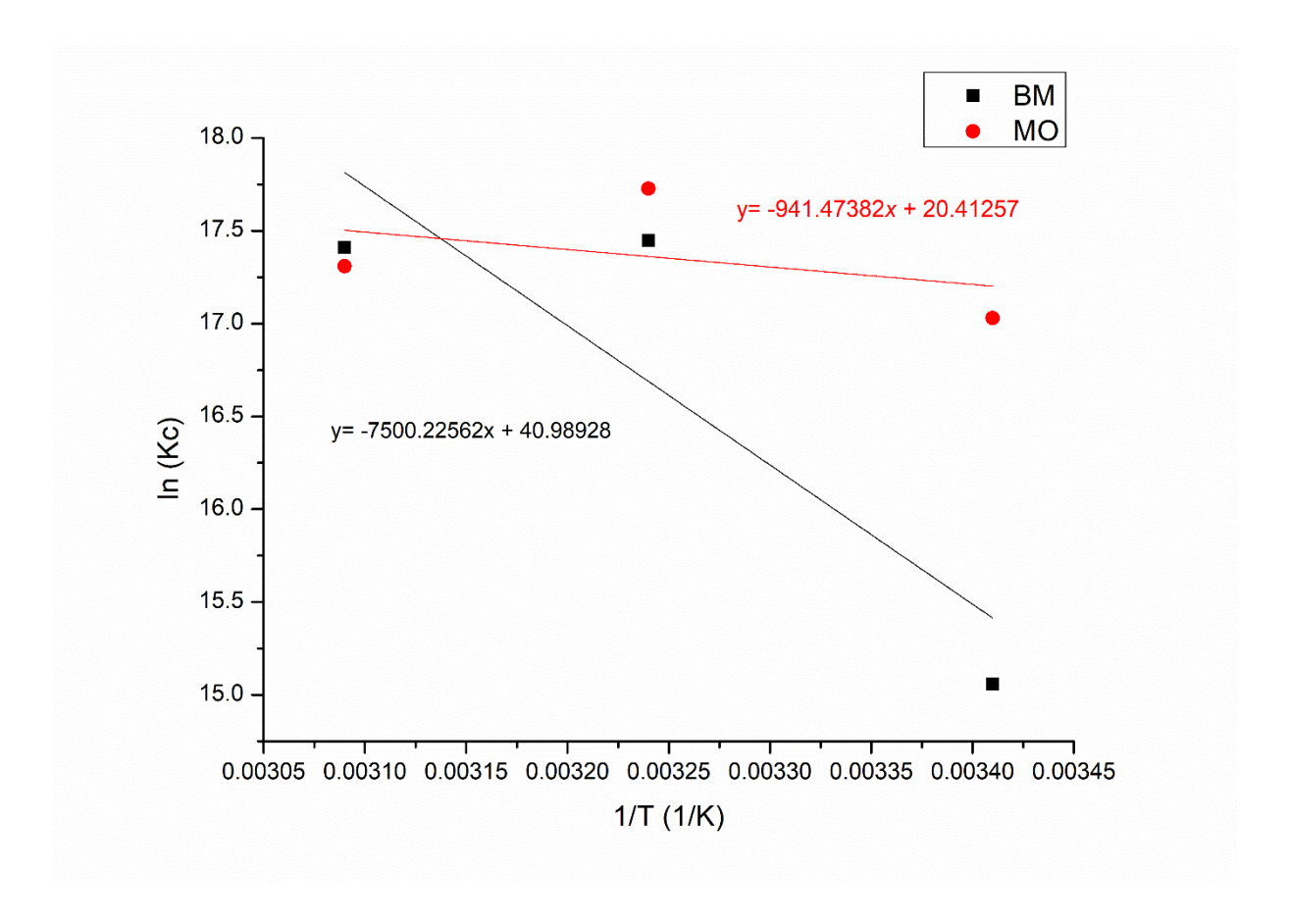


Figure III.11: The thermodynamic curves of the BM and MO.

Chapter III: Results and Discussion

Table III.4: Thermodynamic parameters of the adsorption of BM and MO on activated carbon.

Dey s	ΔS° (J.mol-1K ⁻¹)	ΔH° (KJ.mol ⁻¹)		\mathbb{R}^2		
			293,15 K	308,15 K	323,15 K	
ВМ	0.34062	62.32687	-37.52588	-42.63518	-47.74448	0.5377
МО	0.16962	7.82364	-41.90046	-44.44476	-46.98906	-0.6303

The positive value of ΔH° supports the endothermic nature of MB and MO adsorption on activated carbon, the much higher value for BM suggests that its adsorption is significantly more endothermic than MO, whereas the positive value of ΔS° shows the affinity of activated carbon and the growing randomness at the solid-liquid interface during the adsorption process. It is also worth noting that when temperature rises, Gibbs free energy values fall, allowing adsorbed molecules to diffuse towards the interior pores of the adsorbent particles, and suggesting that higher temperatures favor adsorption.

General conclusion

General conclusion

This work is part of water treatment research, and it focuses on improving the adsorption process for removing chemical pollutants from polluted water. This study focuses on the production of activated carbon and its use in adsorption processes. The characteristics of our activated carbon sample were determined, namely:

✓ Infrared spectroscopy (IR) shows that there are C=C groups indicating the presence of an aromatic ring, C−O characteristic of an epoxide structure or aromatic ethers, and C− H in benzene derivatives.

Kinetic analysis revealed that adsorption is fast at the beginning of adsorption process which is 98.75% for BM and 93.28% for MO, half an hour for BM and MO which is (99.98% of BM) and (99.53% of MO) becomes slower due to saturation of the adsorbent surface. The second order model is favorable for the adsorption of BM, and the first model is favorable for the adsorption of MO.

Adsorption isotherm:

- Dye binding to CA follows the Langmuir model, suggesting that dye adsorption to the CA surface is a monolayer adsorption.

Thermodynamic study:

Positive ΔS° readings indicate activated carbon affinity and increased randomness at the solid-liquid interface during adsorption. Positive ΔH values for MB and MO suggest endothermic reactions between the adsorbent and adsorbate.

References:

- [1] A. Ariho, L. Aja, T. Muhammad, L.J.F. Mohammad, Water pollution: causes, impacts and current efforts to address the issues of water pollution along river Meizimera-kihihi, Kanugu District, Uganda, 13 (2024) 1298.
- [2] P. Chowdhary, R.N. Bharagava, S. Mishra, N.J.E.c. Khan, w. sustainable development: Volume 1: Air, e. resources, Role of industries in water scarcity and its adverse effects on environment and human health, (2020) 235-256.
- [3] T. Krithiga, S. Sathish, A.A. Renita, D. Prabu, S. Lokesh, R. Geetha, S.K.R. Namasivayam, M.J.S.o.T.T.E. Sillanpaa, Persistent organic pollutants in water resources: Fate, occurrence, characterization and risk analysis, 831 (2022) 154808.
- [4] K.J.W.Q.M. Parris, Impact of agriculture on water pollution in OECD countries: recent trends and future prospects, (2014) 33-52.
- [5] S. Bochynska, A. Duszewska, M. Maciejewska-Jeske, M. Wrona, A. Szeliga, M. Budzik, A. Szczesnowicz, G. Bala, M. Trzcinski, B.J.M. Meczekalski, The impact of water pollution on the health of older people, 185 (2024) 107981.
- [6] B. Chen, M. Wang, M. Duan, X. Ma, J. Hong, F. Xie, R. Zhang, X.J.J.o.C.P. Li, In search of key: Protecting human health and the ecosystem from water pollution in China, 228 (2019) 101-111.
- [7] A.M. Nasir, N. Awang, J. Jaafar, A.F. Ismail, M.H.D. Othman, M.A. Rahman, F. Aziz,
- M.A.M.J.J.o.W.P.E. Yajid, Recent progress on fabrication and application of electrospun nanofibrous photocatalytic membranes for wastewater treatment: A review, 40 (2021) 101878.
- [8] N. Rahmati, M. Rahimnejad, M. Pourali, S.K.J.C. Muallah, I.S. Communications, Effective removal of nickel ions from aqueous solution using multi-wall carbon nanotube functionalized by glycerol-based deep eutectic solvent, 40 (2021) 100347.
- [9] M.J.R.G. Alaqarbeh, A. Chemistry, Adsorption phenomena: definition, mechanisms, and adsorption types: short review, 13 (2021) 43-51.
- [10] I.S. Bădescu, D. Bulgariu, I. Ahmad, L.J.J.o.e.m. Bulgariu, Valorisation possibilities of exhausted biosorbents loaded with metal ions—a review, 224 (2018) 288-297.
- [11] M. Thommes, K. Kaneko, A.V. Neimark, J.P. Olivier, F. Rodriguez-Reinoso, J. Rouquerol, K.S.J.P. Sing, a. chemistry, Physisorption of gases, with special reference to the evaluation of surface area and pore size distribution (IUPAC Technical Report), 87(9-10) (2015) 1051-1069.
- [12] N.M. Aljamali, R. Khdur, I.O.J.I.J.o.T. Alfatlawi, C. Kinetics, Physical and chemical adsorption and its applications, 7(2) (2021) 1-8.
- [13] K.K. Kennedy, K.J. Maseka, M.J.O.J.o.A.S. Mbulo, Selected adsorbents for removal of contaminants from wastewater: towards engineering clay minerals, 8(8) (2018) 355-369.
- [14] A. Hernández-Abreu, S. Álvarez-Torrellas, R. Rocha, M. Pereira, V. Águeda, J. Delgado, M. Larriba, J. García, J.J.A.S.S. Figueiredo, Effective adsorption of the endocrine disruptor compound bisphenol a from water on surface-modified carbon materials, 552 (2021) 149513.
- [15] B.A.A. Alongamo, L.D. Ajifack, J.N. Ghogomu, N.J. Nsami, J.M.J.J.o.C. Ketcha, Activated carbon from the peelings of cassava tubers (Manihot esculenta) for the removal of nickel (II) ions from aqueous solution, 2021(1) (2021) 5545110.
- [16] M.J. Horsfall, A. Arbia, A.J.A.J.o.B. Spiff, Removal of Cu (II) and Zn (II) ions from wastewater by cassava (Manihot esculenta Cranz) waste biomass, 2(10) (2003) 360-364.
- [17] D. Feng, H. Yu, H. Deng, F. Li, C.J.B. Ge, Adsorption characteristics of norfloxacin by biochar prepared by cassava dreg: kinetics, isotherms, and thermodynamic analysis, 10(4) (2015) 6751-6768.
- [18] J. Wu, J. Yang, G. Huang, C. Xu, B.J.J.o.C.P. Lin, Hydrothermal carbonization synthesis of cassava slag biochar with excellent adsorption performance for Rhodamine B, 251 (2020) 119717.
- [19] A. Navya, S. Nandhini, S. Sivamani, G. Vasu, N. Sivarajasekar, A.J.D. Hosseini-Bandegharaei, W. Treatment, Preparation and characterization of cassava stem biochar for mixed reactive dyes removal from simulated effluent, 189 (2020) 440-451.

- [20] W. Li, W. Mo, C. Kang, M. Zhang, M. Meng, M.J.E.C. Chen, Engineering, Adsorption of nitrate from aqueous solution onto modified cassava (Manihot esculenta) straw/Adsorpcja azotanow z roztworu wodnego na zmodyfikowanej slomie manioku Manihot esculenta, 19(4) (2012) 629.
- [21] A. Belcaid, B. Beakou, K. El Hassani, S. Bouhsina, A.J.W.S. Anouar, Technology, Efficient removal of Cr (VI) and Co (II) from aqueous solution by activated carbon from Manihot esculenta Crantz agricultural bio-waste, 83(3) (2021) 556-566.
- [22] M. Horsfall Jr, A.J.W.r. Abia, Sorption of cadmium (II) and zinc (II) ions from aqueous solutions by cassava waste biomass (Manihot sculenta Cranz), 37(20) (2003) 4913-4923.
- [23] X. Qi, X. Tong, W. Pan, Q. Zeng, S. You, J.J.J.o.C.P. Shen, Recent advances in polysaccharide-based adsorbents for wastewater treatment, 315 (2021) 128221.
- [24] M. Musah, J. Yisa, M.T. Suleiman, M. Abdullahi, E.Y. Shaba, Study of isotherm models for the adsorption of cr (vi) ion from aqueous solution onto Bombax buonopozense calyx activated carbon, (2018).
- [25] V.J.C. Bolis, t.m.i. catalysis, Fundamentals in adsorption at the solid-gas interface. Concepts and thermodynamics, (2013) 3-50.
- [26] Y.-S. Ho, G.J.C.e.j. McKay, Sorption of dye from aqueous solution by peat, 70(2) (1998) 115-124.
- [27] C.H. Giles, D. Smith, A.J.J.o.c. Huitson, i. science, A general treatment and classification of the solute adsorption isotherm. I. Theoretical, 47(3) (1974) 755-765.
- [28] K.S.J.P. Sing, a. chemistry, Reporting physisorption data for gas/solid systems with special reference to the determination of surface area and porosity (Provisional), 54(11) (1982) 2201-2218.
- [29] M. Sultan, T. Miyazaki, S.J.R.E. Koyama, Optimization of adsorption isotherm types for desiccant air-conditioning applications, 121 (2018) 441-450.
- [30] P.J.C. Carrott, Adsorption of water vapor by non-porous carbons, 30(2) (1992) 201-205.
- [31] C.J.P.C.C.P. Buttersack, Modeling of type IV and V sigmoidal adsorption isotherms, 21(10) (2019) 5614-5626
- [32] V.J. Inglezakis, S.G. Poulopoulos, H.J.M. Kazemian, M. Materials, Insights into the S-shaped sorption isotherms and their dimensionless forms, 272 (2018) 166-176.
- [33] M.A. Al-Ghouti, D.A.J.J.o.h.m. Da'ana, Guidelines for the use and interpretation of adsorption isotherm models: A review, 393 (2020) 122383.
- [34] E.F. Covelo, F.A. Vega, M.L.J.J.o.H.M. Andrade, Heavy metal sorption and desorption capacity of soils containing endogenous contaminants, 143(1-2) (2007) 419-430.
- [35] R. Juang, F. Wu, R.J.E.T. Tseng, The ability of activated clay for the adsorption of dyes from aqueous solutions, 18(5) (1997) 525-531.
- [36] D. Manohar, B. Noeline, T.J.A.C.S. Anirudhan, Adsorption performance of Al-pillared bentonite clay for the removal of cobalt (II) from aqueous phase, 31(3-4) (2006) 194-206.
- [37] H.K. Boparai, M. Joseph, D.M.J.E.S. O'Carroll, P. Research, Cadmium (Cd 2+) removal by nano zerovalent iron: surface analysis, effects of solution chemistry and surface complexation modeling, 20 (2013) 6210-6221.
- [38] M.A. Alsharif, Understanding Adsorption: Theories, Techniques, and Applications, (2025).
- [39] T. Odetoye, M.A. Bakar, J.J.N.J.o.T.D. Titiloye, Pyrolysis and characterization of Jatropha curcas shell and seed coat, 16(2) (2019) 71-77.
- [40] N. Radenahmad, A.T. Azad, M. Saghir, J. Taweekun, M.S.A. Bakar, M.S. Reza, A.K.J.R. Azad, S.E. Reviews, A review on biomass derived syngas for SOFC based combined heat and power application, 119 (2020) 109560.
- [41] X. Yang, Y. Wan, Y. Zheng, F. He, Z. Yu, J. Huang, H. Wang, Y.S. Ok, Y. Jiang, B.J.C.E.J. Gao, Surface functional groups of carbon-based adsorbents and their roles in the removal of heavy metals from aqueous solutions: a critical review, 366 (2019) 608-621.
- [42] K.S. Ukanwa, K. Patchigolla, R. Sakrabani, E. Anthony, S.J.S. Mandavgane, A review of chemicals to produce activated carbon from agricultural waste biomass, 11(22) (2019) 6204.
- [43] M.A. Yahya, Z. Al-Qodah, C.Z.J.R. Ngah, s.e. reviews, Agricultural bio-waste materials as potential sustainable precursors used for activated carbon production: A review, 46 (2015) 218-235.

- [44] P.J.R. González-García, s.e. reviews, Activated carbon from lignocellulosics precursors: A review of the synthesis methods, characterization techniques and applications, 82 (2018) 1393-1414.
- [45] M. Alhinai, A.K. Azad, M.A. Bakar, N.J.I.J.R.E.R. Phusunti, Characterisation and thermochemical conversion of rice husk for biochar production, 8(3) (2018) 1648-1656.
- [46] T. Odetoye, T. Afolabi, M. Abu Bakar, J.J.E. Titiloye, Ecology, Environment, Thermochemical characterization of Nigerian Jatropha curcas fruit and seed residues for biofuel production, 3 (2018) 330-337.
- [47] Z.Z. Chowdhury, S.B.A. Hamid, R. Das, M.R. Hasan, S.M. Zain, K. Khalid, M.N.J.B. Uddin, Preparation of carbonaceous adsorbents from lignocellulosic biomass and their use in removal of contaminants from aqueous solution, 8(4) (2013) 6523-6555.
- [48] V. Dhyani, T.J.R.e. Bhaskar, A comprehensive review on the pyrolysis of lignocellulosic biomass, 129 (2018) 695-716.
- [49] S. Afroze, N. Torino, P.F. Henry, M.S. Reza, Q. Cheok, A.K.J.M.L. Azad, Insight of novel layered perovskite PrSrMn2O5+ δ: a neutron powder diffraction study, 261 (2020) 127126.
- [50] D. Mohan, A. Sarswat, Y.S. Ok, C.U.J.B.t. Pittman Jr, Organic and inorganic contaminants removal from water with biochar, a renewable, low cost and sustainable adsorbent—a critical review, 160 (2014) 191-202.
- [51] W. Ao, J. Fu, X. Mao, Q. Kang, C. Ran, Y. Liu, H. Zhang, Z. Gao, J. Li, G.J.R. Liu, S.E. Reviews, Microwave assisted preparation of activated carbon from biomass: A review, 92 (2018) 958-979.
- [52] E. Menya, P.W. Olupot, H. Storz, M. Lubwama, Y.J.C.E.R. Kiros, Design, Production and performance of activated carbon from rice husks for removal of natural organic matter from water: a review, 129 (2018) 271-296.
- [53] N.A. Rashidi, S.J.C.E.J. Yusup, A review on recent technological advancement in the activated carbon production from oil palm wastes, 314 (2017) 277-290.
- [54] H.W. Lee, Y.-M. Kim, S. Kim, C. Ryu, S.H. Park, Y.-K.J.C.I. Park, Review of the use of activated biochar for energy and environmental applications, 26 (2018) 1-10.
- [55] H.H. Rafsanjani, H. Kamandari, H.J.I.J.C.E. Najjarzadeh, Study on pore and surface development of activated carbon produced from Iranian coal in a rotary kiln reactor, 10(3) (2013) 27-38.
- [56] J. Alvarez, G. Lopez, M. Amutio, J. Bilbao, M.J.I. Olazar, E.C. Research, Physical activation of rice husk pyrolysis char for the production of high surface area activated carbons, 54(29) (2015) 7241-7250.
- [57] S. Wong, N. Ngadi, I.M. Inuwa, O.J.J.o.C.P. Hassan, Recent advances in applications of activated carbon from biowaste for wastewater treatment: a short review, 175 (2018) 361-375.
- [58] A. El-Naggar, S.S. Lee, J. Rinklebe, M. Farooq, H. Song, A.K. Sarmah, A.R. Zimmerman, M. Ahmad, S.M. Shaheen, Y.S.J.G. Ok, Biochar application to low fertility soils: A review of current status, and future prospects, 337 (2019) 536-554.
- [59] M.S. Reza, C.S. Yun, S. Afroze, N. Radenahmad, M.S.A. Bakar, R. Saidur, J. Taweekun, A.K.J.A.J.o.B. Azad, A. Sciences, Preparation of activated carbon from biomass and its' applications in water and gas purification, a review, 27(1) (2020) 208-238.
- [60] M.A. Yahya, M.H. Mansor, W.A.A.W. Zolkarnaini, N.S. Rusli, A. Aminuddin, K. Mohamad, F.A.M. Sabhan, A.A.A. Atik, L.N. Ozair, A brief review on activated carbon derived from agriculture byproduct, AIP conference proceedings, AIP Publishing, 2018.
- [61] M.I. Din, S. Ashraf, A.J.S.p. Intisar, Comparative study of different activation treatments for the preparation of activated carbon: a mini-review, 100(3) (2017) 299-312.
- [62] N.D. Mu'azu, N. Jarrah, M. Zubair, O.J.I.j.o.e.r. Alagha, p. health, Removal of phenolic compounds from water using sewage sludge-based activated carbon adsorption: a review, 14(10) (2017) 1094.
- [63] Q. Cao, K.-C. Xie, Y.-K. Lv, W.-R.J.B.T. Bao, Process effects on activated carbon with large specific surface area from corn cob, 97(1) (2006) 110-115.
- [64] N. Isoda, R. Rodrigues, A. Silva, M. Gonçalves, D. Mandelli, F.C.A. Figueiredo, W.A.J.P.T. Carvalho, Optimization of preparation conditions of activated carbon from agriculture waste utilizing factorial design, 256 (2014) 175-181.

- [65] M.A.A. Zaini, M.J.J.J.o.a. Kamaruddin, a. pyrolysis, Critical issues in microwave-assisted activated carbon preparation, 101 (2013) 238-241.
- [66] B. Caglar, B. Afsin, E. Koksal, A. Tabak, E.J.Q.N. Eren, Characterization of Unye bentonite after treatment with sulfuric acid, 36 (2013) 955-959.
- [67] A. Arami-Niya, W. Wan Daud, F. Mjalli, Production of palm shell-based activated carbon with more homogeniouse pore size distribution, (2010).
- [68] A. Arami-Niya, W.M.A.W. Daud, F.S.J.C.E.R. Mjalli, Design, Comparative study of the textural characteristics of oil palm shell activated carbon produced by chemical and physical activation for methane adsorption, 89(6) (2011) 657-664.
- [69] T. Lee, Z.A. Zubir, F.M. Jamil, A. Matsumoto, F.-Y.J.J.o.A. Yeoh, A. Pyrolysis, Combustion and pyrolysis of activated carbon fibre from oil palm empty fruit bunch fibre assisted through chemical activation with acid treatment, 110 (2014) 408-418.
- [70] H.S. Min, M. Abbas, R. Kanthasamy, H.A. Aziz, T.C.J.I.i.E.-p.P.L. Chay, Activated carbon: prepared from various precursors, (2017) 1-20.
- [71] M. Danish, R. Hashim, M.M. Ibrahim, M. Rafatullah, O.J.J.o.A. Sulaiman, A. Pyrolysis, Surface characterization and comparative adsorption properties of Cr (VI) on pyrolysed adsorbents of Acacia mangium wood and Phoenix dactylifera L. stone carbon, 97 (2012) 19-28.
- [72] A. Arami-Niya, W.M.A.W. Daud, F.S. Mjalli, F. Abnisa, M.S.J.C.e.r. Shafeeyan, design, Production of microporous palm shell based activated carbon for methane adsorption: modeling and optimization using response surface methodology, 90(6) (2012) 776-784.
- [73] R.-L. Tseng, S.-K. Tseng, F.-C.J.C. Wu, S.A. Physicochemical, E. Aspects, Preparation of high surface area carbons from Corncob with KOH etching plus CO2 gasification for the adsorption of dyes and phenols from water, 279(1-3) (2006) 69-78.
- [74] T. Ahmad, M.J.J.o.e.m. Danish, Prospects of banana waste utilization in wastewater treatment: A review, 206 (2018) 330-348.
- [75] R.H. Hesas, W.M.A.W. Daud, J. Sahu, A.J.J.o.A. Arami-Niya, A. pyrolysis, The effects of a microwave heating method on the production of activated carbon from agricultural waste: A review, 100 (2013) 1-11.
- [76] T.M. Alslaibi, I. Abustan, M.A. Ahmad, A.A.J.J.o.C.T. Foul, Biotechnology, A review: production of activated carbon from agricultural byproducts via conventional and microwave heating, 88(7) (2013) 1183-1190.
- [77] P.D. Pathak, S.A.J.J.o.E.C.E. Mandavgane, Preparation and characterization of raw and carbon from banana peel by microwave activation: Application in citric acid adsorption, 3(4) (2015) 2435-2447.
- [78] D. Angın, E. Altintig, T.E.J.B.T. Köse, Influence of process parameters on the surface and chemical properties of activated carbon obtained from biochar by chemical activation, 148 (2013) 542-549.
- [79] J. Rivera-Utrilla, M. Sánchez-Polo, M.Á. Ferro-García, G. Prados-Joya, R.J.C. Ocampo-Pérez, Pharmaceuticals as emerging contaminants and their removal from water. A review, 93(7) (2013) 1268-1287.
- [80] A.E. Burakov, E.V. Galunin, I.V. Burakova, A.E. Kucherova, S. Agarwal, A.G. Tkachev, V.K.J.E. Gupta, e. safety, Adsorption of heavy metals on conventional and nanostructured materials for wastewater treatment purposes: A review, 148 (2018) 702-712.
- [81] J. Wang, F. Wu, M. Wang, N. Qiu, Y. Liang, S. Fang, X.J.A.J.o.B. Jiang, Preparation of activated carbon from a renewable agricultural residue of pruning mulberry shoot, 9(19) (2010) 2762-2767.
- [82] C. Namasivayam, D.J.B.t. Sangeetha, Removal of molybdate from water by adsorption onto ZnCl2 activated coir pith carbon, 97(10) (2006) 1194-1200.
- [83] C. Namasivayam, D.J.C. Sangeetha, Kinetic studies of adsorption of thiocyanate onto ZnCl2 activated carbon from coir pith, an agricultural solid waste, 60(11) (2005) 1616-1623.
- [84] A.A. Oladipo, A.O.J.J.o.e.m. Ifebajo, Highly efficient magnetic chicken bone biochar for removal of tetracycline and fluorescent dye from wastewater: two-stage adsorber analysis, 209 (2018) 9-16.

- [85] J. Salman, F.J.J.E.A.C. Hussein, Batch adsorber design for different solution volume/adsorbate mass ratios of bentazon, carbofuran and 2, 4-D adsorption on to date seeds activated carbon, 2(120) (2014) 2.
- [86] S. Afroze, A. Binti Haji Bakar, M.S. Reza, M. Salam, A.K. Azad, Polyvinylidene fluoride (PVDF) piezoelectric energy harvesting from rotary retracting mechanism: imitating forearm motion, 7th Brunei International Conference on Engineering and Technology 2018 (BICET 2018), IET, 2018, p. 94. [87] M.A. Hossain, S. Shams, M. Amin, M.S. Reza, T.U.J.B. Chowdhury, Perception and barriers to implementation of intensive and extensive green roofs in Dhaka, Bangladesh, 9(4) (2019) 79. [88] A.E. Ogungbenro, D.V. Quang, K. Al-Ali, M.R.J.E.P. Abu-Zahra, Activated carbon from date seeds for CO2 capture applications, 114 (2017) 2313-2321.
- [89] H. Lei, Z. Chen, J. Zhang, W.J.S. Yu, P. Technology, Ti3C2Tx MXene-assisted solar-driven CO2 adsorption and photothermal regeneration over mesoporous SiO2, 347 (2024) 127537. [90] P. Sharma, H. Kaur, M. Sharma, V.J.E.m. Sahore, assessment, A review on applicability of naturally available adsorbents for the removal of hazardous dyes from aqueous waste, 183 (2011)
- [91] A.M. Elsayed, A.A. Askalany, A.D. Shea, H.J. Dakkama, S. Mahmoud, R. Al-Dadah, W.J.R. Kaialy, S.E. Reviews, A state of the art of required techniques for employing activated carbon in renewable energy powered adsorption applications, 79 (2017) 503-519.